Engineering oxygen-independent biotin biosynthesis in Saccharomyces cerevisiae

Wronska, Anna K.; van den Broek, Marcel; Perli, Thomas; de Hulster, Erik; Pronk, Jack T.; Daran, Jean Marc

DOI
10.1016/j.ymben.2021.05.006

Publication date
2021

Document Version
Accepted author manuscript

Published in
Metabolic Engineering

Engineering oxygen-independent biotin biosynthesis in *Saccharomyces cerevisiae*

Anna K. Wronska, Marcel van den Broek, Thomas Perli, Erik de Hulster, Jack T. Pronk, Jean-Marc Daran*

Department of Biotechnology, Delft University of Technology, Van der Maasweg 9, 2629 HZ Delft, The Netherlands.

*Corresponding author: Department of Biotechnology, Delft University of Technology, Van der Maasweg 9, 2629 HZ Delft, The Netherlands. Tel: +31-15-27-82412; E-Mail: J.G.Daran@tudelft.nl

Anna K. Wronska:	a.k.wronska@tudelft.nl	0000-0002-6103-3039
Marcel van den Broek	marcel.vandenbroek@tudelft.nl	
Thomas Perli	t.perli@tudelft.nl	0000-0002-4910-3292
Erik de Hulster	a.f.dehulster@tudelft.nl	
Jack T. Pronk:	j.t.pronk@tudelft.nl	0000-0002-5617-4611
Jean-Marc Daran:	j.g.daran@tudelft.nl	0000-0003-3136-8193

For submission in Metabolic Engineering

Keywords

Prokaryotic pathway, biotin biosynthesis, vitamin B_7, gene dosage, anoxic growth

21 Graphical abstract

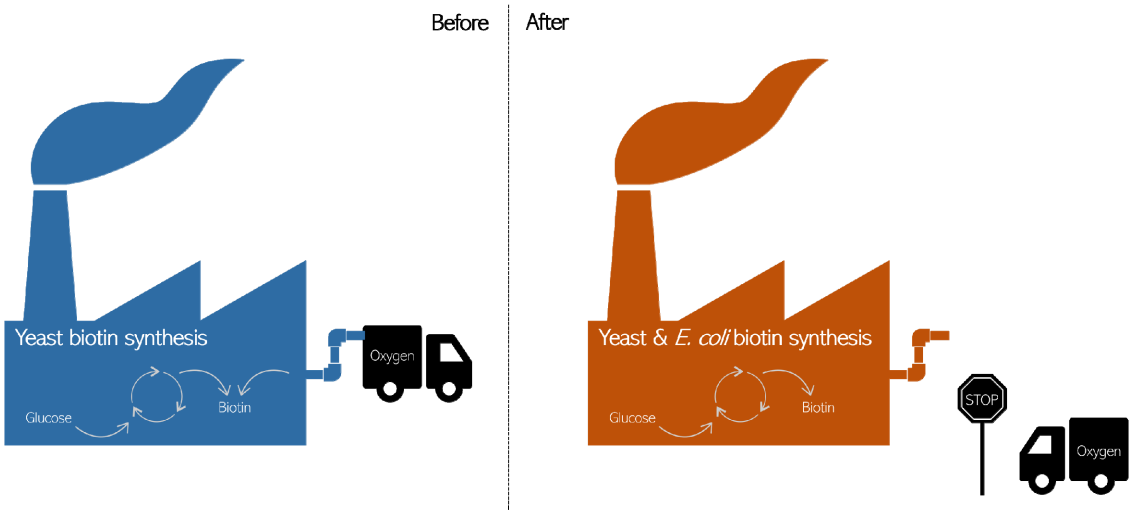

22

23

24

25

Abstract

An oxygen requirement for *de novo* biotin synthesis in *Saccharomyces cerevisiae* precludes the application of biotin-prototrophic strains in anoxic processes that use biotin-free media. To overcome this issue, this study explores introduction of the oxygen-independent *Escherichia coli* biotin-biosynthesis pathway in *S. cerevisiae*. Implementation of this pathway required expression of seven *E. coli* genes involved in fatty-acid synthesis and three *E. coli* genes essential for the formation of a pimelate thioester, key precursor of biotin synthesis. A yeast strain expressing these genes readily grew in biotin-free medium, irrespective of the presence of oxygen. However, the engineered strain exhibited specific growth rates 25% lower in biotin-free media than in biotin-supplemented media. Following adaptive laboratory evolution in anoxic cultures, evolved cell lines that no longer showed this growth difference in controlled bioreactors, were characterized by genome sequencing and proteome analyses. The evolved isolates exhibited a whole-genome duplication accompanied with an alteration in the relative gene dosages of biosynthetic pathway genes. These alterations resulted in a reduced abundance of the enzymes catalyzing the first three steps of the *E. coli* biotin pathway. The evolved pathway configuration was reverse engineered in the diploid industrial *S. cerevisiae* strain Ethanol Red. The resulting strain grew at nearly the same rate in biotin-supplemented and biotin-free media non-controlled batches performed in an anaerobic chamber. This study established an unique genetic engineering strategy to enable biotin-independent anoxic growth of *S. cerevisiae* and demonstrated its portability in industrial strain backgrounds.

47 # 1. Introduction

48 Typical industrial substrates derived from plant biomass such as sugarcane juice, starch, and ligno-
49 cellulosic hydrolysates are subjected to harsh physical-chemical treatments that result in lowering
50 nutritional properties (Basso et al., 2008) by affecting stability of vitamins (Brown and Du Vigneaud,
51 1941; Mauri et al., 1989; Saidi and Warthesen, 1983; Schnellbaecher et al., 2019). In these substrates,
52 biotin concentration is ranging from 10 to 80 ppb (Jackson and Macek, 1944; Pejin et al., 1996).
53 Preloading of cells with vitamins during biomass propagation (van Dijk et al., 2020) or supplementing
54 vitamins during fermentation showed positive impact on yeast fermentation performance (Alfenore et
55 al., 2002; Brandberg et al., 2007; Brandberg et al., 2005) and significantly reduced occurrences of stuck
56 wine fermentations (Bohlscheid et al., 2007; Medina et al., 2012). Thus, the estimation and the provision
57 of the proper nutritional requirements of a microbial strain for industrial application are key points to
58 improve robustness of a fermentation process (Hahn-Hagerdal et al., 2005). In this context, vitamin
59 prototrophic yeast strains could be highly beneficial.

60 Although most *S. cerevisiae* strains harbor all genes necessary to encode all known enzymes of the biotin
61 biosynthesis pathway, these strains are bradytroph for biotin, exhibiting very low growth on media
62 devoid of biotin. Evolutionary engineering and rational metabolic engineering strategies led to the
63 selection of yeast strains whose growth in biotin-free medium was as fast as the growth of the reference
64 strain in the presence of biotin (Bracher et al., 2017; Wronska et al., 2020). But in both cases, acquisition
65 of the biotin prototroph phenotype was restricted to the presence of oxygen (Wronska et al., 2020).

66 Several essential carboxylation reactions in eukaryotes and prokaryotes require biotin as a cofactor (Perli
67 et al., 2020c). Despite its essentiality for prototrophic growth, *de novo* synthesis of biotin is restricted to
68 bacteria and a limited number of plant and fungal species. The well-studied biochemical reactions
69 involved in assembly of the fused heterocyclic rings of biotin are conserved among yeasts, bacteria and
70 plants (Patton et al., 1998). This assembly pathway starts with a thioester of either coenzyme A (CoA)
71 or acyl carrier protein (Acp) with the 7-carbon dicarboxylic acid pimelate. This thioester is then further
72 converted in four successive enzymatic steps catalyzed by 8-amino-7-oxononaote (7-keto-8-
73 aminopelargonic acid, KAPA) synthase (EC 2.3.1.47), 7,8-diamino-nonanoate (DAPA) synthase (EC

74 2.6.1.62), dethiobiotin synthetase (EC 6.3.3.3) and biotin synthase (EC 2.8.1.6) to finally yield biotin
75 (Streit and Entcheva, 2003). Recently, a novel reaction involved in biotin synthesis was reported for
76 cyanobacteria. In this reaction, the single-turnover suicide enzyme BioU converts KAPA to DAPA,
77 using its Lys124 residue as an amino donor (Sakaki et al., 2020) (Figure 1).

78 The pathway for synthesis of the pimeloyl thioester that contributes to the valerate side chain of biotin
79 is much less conserved and the origin of the pimeloyl moiety in eukaryotes remains elusive. The recent
80 characterization of Bio1 from *Cyberlindnera fabianii* and *Saccharomyces cerevisiae,* an enzyme whose
81 activity remains unresolved but which is essential for pimeloyl-thioester formation in yeast (Hall and
82 Dietrich, 2007), revealed that it catalyzes an oxygen-dependent reaction (Wronska et al., 2020). A
83 similar oxygen dependency has been reported for the *Bacillus subtilis* P450-enzyme BioI (Figure 1),
84 which performs oxidative cleavage of ACP-bound long-chain fatty and thereby generates pimeloyl-
85 thioester for biotin synthesis (Stok and De Voss, 2000). Expression of *C. fabianii* Bio1 conferred full
86 biotin prototrophy to oxic cultures of multiple laboratory and industrial strains of *S. cerevisiae* (Wronska
87 et al., 2020). However, due to the oxygen dependence of this enzyme, this strategy is not applicable in
88 large-scale anoxic processes such as the yeast-based production of ethanol and isobutanol.

89 Prokaryotic metabolism offers options for pimeloyl-thioester biosynthesis that are independent of
90 molecular oxygen and might be suitable for implementation in *S. cerevisiae* to meet biotin demands in
91 processes performed in absence of oxygen. In *B. subtilis*, pimeloyl-CoA can be formed by BioW, a
92 pimeloyl-CoA synthetase that converts free pimelic acid to pimeloyl-CoA in presence of ATP and free
93 CoA (Bower et al., 1996). The substrate of BioW, pimelic acid (heptanedioic acid), has been proposed
94 to be derived from fatty acid synthesis (Manandhar and Cronan, 2017). In *Escherichia coli*, a divergent
95 pathway for pimelate thioester synthesis has been elucidated (Lin et al., 2010). This pathway is
96 intertwined with fatty acid synthesis and is initiated by SAM-dependent methylation of malonyl-CoA
97 by the malonyl-[Acp] O-methyltransferase encoded by *bioC*, yielding malonyl-CoA or malonyl-[Acp])
98 (Lin and Cronan, 2012). The methyl group of malonyl-CoA methyl ester mimics the methyl ends of
99 fatty acyl chains and removes the charge of the carboxyl group. Malonyl-CoA methyl ester then
100 undergoes two cycles of chain elongation by a modified type-II fatty acid synthesis pathway involving

101 FabB, a 3-oxoacyl-[Acp]-synthase (EC 2.3.1.41), as well as FabI (EC 1.3.1.9), FabZ (EC 4.2.1.59) and
102 FabG (EC 1.1.1.100), which produce methyl pimeloyl-[Acp]. In a final step, BioH, a pimeloyl-[Acp]
103 methyl esterase, removes the methyl group from pimeloyl-[Acp] methyl ester, thus preventing further
104 elongation (Agarwal et al., 2012). The released pimeloyl-[Acp] is then used by BioF, the first enzyme
105 of the canonical pathway for formation of the hetero-bi-cyclic ring of biotin, which is an homolog of *S.*
106 *cerevisiae* Bio6. BioF produces KAPA, which is the link between all hitherto described pathways for *de*
107 *novo* syntheses of biotin. KAPA can be converted to biotin by DAPA synthase (Bio3, BioA) (or, in
108 cyanobacteria, by (S)-8-amino-7-oxononanoate synthase BioU (Sakaki et al., 2020), dethiobiotin
109 synthetase (Bio4, BioU) and biotin synthase (Bio2, BioB) (Otsuka et al., 1988) (Figure 1).

110 Since the multi-step prokaryotic pathway for biotin synthesis via malonyl-CoA methyl ester is not
111 known to involve oxygen-requiring enzymes, its introduction into *S. cerevisiae* provides a possible
112 strategy for *de novo* synthesis of biotin in anoxicc cultures. To investigate this strategy, the *E. coli* genes
113 encoding enzymes involved in KAPA synthesis, comprising *fabD*, *bioC*, *fabB*, *fabG*, *fabZ*, *fabI*, *bioH*,
114 *bioF*, *acpP* and *acpS*, were expressed in *S. cerevisiae*. Individual transformants were evolved for fast
115 growth in biotin-free medium conditions in absence of oxygen. Evolved biotin-prototrophic lineages
116 were characterized by whole-genome re-sequencing and observed genetic changes were reverse
117 engineered into *S. cerevisiae* Ethanol Red, a commercial yeast strain applied in industrial bioethanol
118 production processes.

119

120

121 # 2. Materials and Methods

122 ## 2.1 Strains, media and maintenance

123 The *S. cerevisiae* strains used in this study are derived from the CEN.PK (Entian and Kotter, 2007;
124 Salazar et al., 2017) and Ethanol Red lineages (Leaf, Lesaffre, Marcq-en-Baroeul, France) (Table 1).
125 Yeast strains were grown on YP medium (10 g L^{-1} yeast extract [BD Biosciences, Vianen, NL], 20 g L^{-1}
126 peptone [BD Biosciences]) or on chemically defined medium (SM) containing 3.0 g L^{-1} KH_2PO_4,
127 5.0 g L^{-1} $(NH_4)_2SO_4$, 0.5 g L^{-1} $MgSO_4$, 7·H_2O, 1 mL L^{-1} trace element solution, and 1 mL L^{-1} vitamin
128 solution (0.05 g L^{-1} D-(+)-biotin, 1.0 g L^{-1} D-calcium pantothenate, 1.0 g L^{-1} nicotinic acid, 25 g L^{-1}
129 myo-inositol, 1.0 g L^{-1} thiamine hydrochloride, 1.0 g L^{-1} pyridoxol hydrochloride, 0.2 g L^{-1}
130 4-aminobenzoic acid) (Verduyn et al., 1992). The pH was adjusted to 6 with 2 M KOH prior to
131 autoclaving at 121 ºC for 20 min. Vitamin solutions were sterilized by filtration and added to the sterile
132 medium. Concentrated sugar solutions were autoclaved at 110 ºC for 20 min and added to the sterile
133 medium to give a final concentration of 20 g L^{-1} glucose (YPD and SMD). Biotin-free SM was prepared
134 similarly, but biotin was omitted from the vitamin solution (1.0 g L^{-1} D-calcium pantothenate, 1.0 g L^{-1}
135 nicotinic acid, 25 g L^{-1} myo-inositol, 1.0 g L^{-1} thiamine hydrochloride, 1.0 g L^{-1} pyridoxol
136 hydrochloride, 0.2 g L^{-1} 4-aminobenzoic acid) (Bracher et al., 2017). Similarly, after autoclaving
137 concentrated glucose solution at 110 ºC for 20 min, glucose was added to biotin-free SM to a final
138 concentration of 20 g L^{-1} (biotin-free SMD). Solid media contained 2% (w/v) Bacto agar (BD
139 Biosciences) and, when indicated, acetamide for SMD acetamide (20 g L^{-1} glucose, 1.2 g L^{-1} acetamide,
140 3.0 g L^{-1} KH_2PO_4, 6.6 g L^{-1} K_2SO_4, 0.5 g L^{-1} $MgSO_4$ 7·H_2O, 1 mL L^{-1} trace element solution and 1 mL
141 L^{-1} vitamin solution) (Solis-Escalante et al., 2013), 200 mg L^{-1} hygromycin for YPD hygromycin and
142 200 mg L^{-1} G418 (geneticin) for YPD geneticin. Where indicated, unsaturated fatty acids and/or sterols
143 were added to autoclaved media as Tween 80 (polyethylene glycol sorbate monooleate, Merck,
144 Darmstadt, Germany) and ergosterol (≥95% pure, Sigma-Aldrich, St. Louis, MO). 800-fold
145 concentrated stock solutions of these "anaerobic" growth factors were prepared as described previously
146 and incubated at 80 °C for 20 min before diluting them in growth medium, yielding final concentrations
147 of 420 mg L^{-1} Tween 80 and 10 mg L^{-1} ergosterol (Dekker et al., 2019).

148 *E. coli* cells (XL1-Blue, Agilent Technologies, Santa Clara, CA) were grown in Lysogeny broth (LB)
149 medium (5.0 g L^{-1} yeast extract, 10 g L^{-1} Bacto trypton [BD Biosciences], 5.0 g L^{-1} NaCl) supplemented
150 with 25 mg L^{-1} chloramphenicol, 100 mg L^{-1} ampicillin or 50 mg L^{-1} kanamycin for selection. Solid LB
151 medium contained 2 % bacto agar.
152 Unless indicated otherwise, stock cultures for strain maintenance were prepared by growing yeast strains
153 on YPD and *E. coli* cultures on LB with appropriate antibiotic markers. After reaching late exponential
154 phase, cultures were complemented with sterile glycerol to a final concentration of 30 % (v/v) and stored
155 at −80 °C as 1 mL aliquots until use.
156

157 ## 2.2 Shake flask cultivations

158 For cultivation experiments for determination of specific growth rates, 1 mL aliquot of a stock culture
159 was inoculated in 100 mL SMD in a 500 mL shake flask and incubated for 20 h at 30 °C. A second
160 100 mL SMD culture was started by inoculating 2 mL of the first shake flask culture. When the second
161 culture reached mid-exponential phase, which corresponded to an optical density at 660 nm (OD_{660}) of
162 3-5, an aliquot was used to inoculate a third culture at an OD_{660} of 0.1-0.3. For biotin-free growth studies,
163 the pre-cultivation steps were performed in biotin-free SMD. Strains *S. cerevisiae* IMX585 and
164 CEN.PK113-7D, which consistently failed to grow on biotin-free SMD in the third culture, were
165 included as negative controls in all growth experiments.
166 Growth was monitored by measuring OD_{660} of accurately diluted culture samples of the third shake-
167 flask culture with a Jenway 7200 Spectrophotometer (Cole-Palmer, Stone, United Kingdom). Specific
168 growth rates were calculated from a minimum number of six data points collected during exponential
169 growth and covering 3-4 doublings of OD_{660}. Specific growth rate was calculated using the equation
170 $X = X_0 e^{\mu t}$ in which μ indicates the exponential growth rate. All oxic shake-flask experiments were
171 carried out as biological duplicates in an Innova shaker incubator (New Brunswick Scientific, Edison,
172 NJ) set at 30°C and 200 rpm. To test if growth rate averages observed for different combinations of
173 strains and medium composition are significantly different, one-way analyses of variance (ANOVA)

174 and Tukey's multiple comparison test with α = 0.05 were performed using GraphPad Prism 8.2.1
175 software (GraphPad Software, Inc., San Diego, CA).
176 For growth profiling under anoxic conditions, the first and second pre-culture were grown in 100 mL
177 SMD or biotin-free SMD in a 500 mL shake flask as described previously. A 200 µL sample of mid-
178 exponential-phase (OD_{660} of 3-5) cells from the second culture was then transferred to a Shel Lab
179 Bactron 300 anaerobic workstation (Sheldon Manufacturing Inc., Cornelius, OR) operated at 30 °C. The
180 gas mixture used for flushing the workspace and air lock consisted of 85 % N_2, 10 % CO_2 and 5 % H_2.
181 An IKA KS 260 Basic orbital shaker platform (Dijkstra Verenigde BV, Lelystad, The Netherlands)
182 placed in the anaerobic chamber was set at 200 rpm. A palladium catalyst for hydrogen-dependent
183 oxygen removal was introduced into the chamber to reduce oxygen contamination. Cultures were grown
184 in 50-mL shake flasks containing 40 mL SMD or biotin-free SMD. Concentrated solutions of ergosterol
185 and/or Tween 80 were added as indicated. Sterile growth media were pre-incubated in the anaerobic
186 chamber for at least 48 h prior to inoculation to allow for removal of oxygen. Growth experiments in
187 the anaerobic chamber were started by inoculating shake flasks, containing SMD or biotin-free SMD,
188 with 200 µL of an exponentially growing oxic pre-culture. Growth was measured by periodic
189 measurements of the OD_{600} with an Ultrospec 10 cell-density meter (Biochrom, Cambridge, UK) placed
190 inside the anaerobic chamber. Strains IMX585 and CEN.PK113-7D grown in SMD without "anaerobic"
191 growth factors were used as controls for absence of oxygen in all anoxic experiments (Dekker et al.,
192 2019). All shake flask experiments were carried out as biological duplicates.
193

194 2.3 Molecular biology techniques

195 DNA fragments were amplified by PCR amplification with Phusion Hot Start II High Fidelity
196 Polymerase (Thermo Fisher Scientific, Landsmeer, The Netherlands) and desalted or PAGE-purified
197 oligonucleotide primers (Sigma-Aldrich) (Table 3). For diagnostic PCR analysis DreamTaq polymerase
198 (Thermo Fisher Scientific) was used according to manufacturers' recommendations. PCR products were
199 separated by gel electrophoresis and, if required, purified with a Zymoclean Gel DNA Recovery kit
200 (Zymo Research, Irvine, CA) or GenElute PCR Clean-Up kit (Sigma-Aldrich). Assembly of DNA

201 fragments was, if not mentioned differently, by Golden Gate cloning based on the Yeast tool kit
202 methodology (Lee et al., 2015). Yeast strains of the CEN.PK lineage were transformed by the lithium
203 acetate (LiAc) method (Gietz and Woods, 2002). *S. cerevisiae* Ethanol Red was transformed using
204 electroporation as previously described (Gorter de Vries et al., 2017). Electroporated cells were plated
205 on selective YPD hygromycin or YPD geneticin (G418) agar medium. Genomic DNA of transformants
206 was isolated using the YeaStar Genomic DNA kit (Zymo Research) or with the SDS/LiAc protocol
207 (Looke et al., 2011). *E. coli* cells were chemically transformed (Inoue et al., 1990) and plated on selective
208 LB agar. Plasmids from selected clones were isolated from *E. coli* with a Sigma GenElute Plasmid kit
209 (Sigma-Aldrich) and verified by restriction analysis (Thermo Fisher Scientific) according to the
210 manufacturer's recommendations or by diagnostic PCR.

211

212 2.4 Plasmid construction

213 2.4.1 Construction of part plasmids using Yeast tool kit

214 Coding sequences of *EcfabD, EcbioC, EcfabB, EcfabG, EcfabZ, EcfabI, EcbioH, EcbioF, EcacpP* and
215 *EcacpS* were codon optimized for expression in *S. cerevisiae* using JCat (Grote et al., 2005) and
216 synthesized by GeneArt (Thermo Fisher Scientific). *E. coli* cells were chemically transformed with the
217 plasmids harbouring the coding sequences together with 5' and 3' flanks compatible with the YTK type
218 3 BsaI sites (Lee et al., 2015) and after selection for the antibiotic marker stored as Yeast Tool Kit type
219 plasmids pUD671, pUD663, pUD664, pUD665, pUD666, pUD667, pUD668, pUD669, pUD661,
220 pUD662 (Table 2).

221 The promoter sequence *ScPFK2*p was obtained by PCR application from genomic DNA of CEN.PK113-
222 7D using primer pair 9630/9631. The promoter sequence was introduced in the entry vector pUD565
223 (Hassing et al., 2019) using BsmBI-T4 ligase directed Golden Gate cloning resulting in Yeast Tool Kit
224 type 2 plasmids pGGkp031. Correct assembly was confirmed by restriction analysis with enzyme PvuII
225 (Thermo Fisher Scientific) according to manufacturer's recommendations. The Yeast Tool Kit type
226 plasmid was propagated in *E. coli* grown in liquid LB chloramphenicol at 37 °C and stored at -80 °C.

227 The terminator sequences *ScFBA1*t, *ScTPI1*t and *ScPGI1*t were obtained by PCR with primer
228 combinations 10757/10758, 10765/10766 and 10771/10772, respectively using genomic DNA of *S.*
229 *cerevisiae* CEN.PK113-7D as template. The terminator sequences were cloned in pUD565 using
230 BsmBI-T4 DNA ligase directed Golden Gate cloning yielding the Yeast Tool Kit type 4 plasmids
231 pGGkp046, pGGkp042 and pGGkp044 respectively. After assembly and transformation into *E. coli*,
232 plasmids harbouring the terminator sequences were confirmed by restriction analysis with enzyme SspI
233 (Thermo Fisher Scientific) according to manufacturer's recommendations. The Yeast Tool Kit type
234 plasmids were stored in transformed *E. coli* cultures.

235 The promoter sequence *ScHXK2*p was synthesized by GeneArt (Thermo Fisher Scientific) and is
236 harboured by Yeast Tool Kit type 2 plasmid pGGkp096. The Yeast Tool Kit type plasmid was
237 propagated in a chemically transformed *E. coli* cultures in liquid LB chloramphenicol medium grown at
238 37 °C on a rotary shaker and subsequently stored at -80 °C.

239 2.4.2 Construction of gRNA-expressing plasmid pUDR791

240 The $gRNA_{EcBIOF}$ expressing plasmid pUDR791 was constructed *in vitro* by Gibson assembly. The
241 linearized pROS11 plasmid, obtained by PCR with 6005/6006 was assembled with a PCR amplified
242 fragment using primer 18409 and pROS11 as a template (Mans et al., 2015). Plasmid DNA was isolated
243 from *E. coli* and correct assembly of plasmid pUDR791 was confirmed by diagnostic PCR with primers
244 18457/3841/5941.

245 2.4.3 Construction of expression cassettes

246 The *E. coli fabD* expression cassette was constructed by BsaI–T4 DNA ligase directed Golden Gate
247 cloning combining DNA fragments with compatible overhangs from plasmids pGGkd015, pGGkp062,
248 pUD671, pGGkp037 yielding plasmid pUD978. The next expression plasmids were constructed
249 following a similar cloning principle. The *E. coli bioC* expression cassette was constructed by combining
250 DNA fragments with compatible overhangs from plasmids pGGkd015, pGGkp063, pUD663,
251 pGGkp038 yielding plasmid pUD979. The *E. coli fabB* expression cassette was constructed by
252 combining DNA fragments with compatible overhangs from plasmids pGGkd015, pGGkp064, pUD664,

253 pGGkp040 yielding plasmid pUD980. The *E. coli fabG* expression cassette was constructed by
254 combining DNA fragments with compatible overhangs from plasmids pGGkd015, pGGkp065, pUD665,
255 pGGkp046 yielding plasmid pUD981. The *E. coli fabZ* expression cassette was constructed by
256 combining DNA fragments with compatible overhangs from plasmids pGGkd015, pGGkp074, pUD666,
257 pGGkp045 yielding plasmid pUD982. The *E. coli fabI* expression cassette was constructed by
258 combining DNA fragments with compatible overhangs from plasmids pGGkd015, pGGkp028, pUD667,
259 pGGkp103 yielding plasmid pUD983. The *E. coli bioH* expression cassette was constructed by
260 combining DNA fragments with compatible overhangs from plasmids pGGkd015, pGGkp117, pUD668,
261 pGGkp044 yielding plasmid pUD984. The *E. coli bioF* expression cassette was constructed by
262 combining DNA fragments with compatible overhangs from plasmids pGGkd015, pGGkp031, pUD669,
263 pGGkp042 yielding plasmid pUD985. The *E. coli acpP* expression cassettee was constructed by
264 combining DNA fragments with compatible overhangs from plasmids pGGkd015, pGGkp033, pUD661,
265 pGGkp048 yielding plasmid pUD986. The *E. coli acpS* expression cassette was constructed by
266 combining DNA fragments with compatible overhangs from plasmids pGGkd015, pGGkp096, pUD662,
267 pGGkp041 yielding plasmid pUD987.

268 After assembly reaction and transformation of *E. coli* with the plasmids carrying the expression
269 cassettes, four to eight colonies were selected for each plasmid, followed by isolation of plasmid DNA.
270 Correct assembly was checked by diagnostic PCR primer combinations, with one primer binding outside
271 the expression cassette and one within the gene sequence: 13483/12761 for *EcfabD,* 10320/10325 for
272 *EcbioC,* 13483/12745 for *EcfabB,* 13483/12751 for *EcfabG,* 13483/12759 for *EcfabZ,* 13483/12763 for
273 *EcfabI,* 10320/10325 for *EcbioH,* 13483/13283 for *EcbioF,* 10320/10325 for *EcacpP* and 13483/12749
274 for *EcacpS.* The obtained plasmids were stored as pUD979, pUD980, pUD981, pUD982, pUD983,
275 pUD984, pUD985, pUD986, pUD987.

276

277 ## 2.5 Strain construction

278 ### 2.5.1 Integration of *E. coli bio* gene expression cassettes into *S. cerevisiae*

279 *S. cerevisiae* IMX2600 was constructed by homology-directed repair by assembly and integration of
280 two cassettes containing *Spycas9* and the natNT2 marker into the *CAN1* locus as described in (Mans et
281 al., 2015). The *EcbioC, EcbioH* and *EcbioF* expression cassettes were PCR-amplified with the following
282 primer pairs adding 60-bp homologous sequences (Kuijpers et al., 2013a): 18406/18405 for *EcbioC*
283 (pUD979), 12455/12450 for *EcbioH* (pUD984) and 14448/18404 for *EcbioF* (pUD985). Targeting at
284 the *ScSGA1* locus in IMX2600 was directed by Cas9 activity and a target-specific gRNA expressing
285 plasmid. The strain was co-transformed with the *EcbioC, EcbioH* and *EcbioF* expression cassette
286 fragments and the plasmid pUDR119 expressing the gRNA to target Cas9 activity to the *ScSGA1* locus
287 (Papapetridis et al., 2018) using the LiAc transformation protocol. Transformed cells were plated on
288 selective SMD with acetamide and incubated for 3 days at 30 °C. Genomic DNA of colonies was isolated
289 and the desired genotype confirmed by diagnostic PCR using primer combinations 11898/13545,
290 13284/13281, 13280/13283 and 1719/11899. A verified clone was inoculated in 20 mL non-selective
291 YPD for plasmid removal and incubated for 24 h at 30 °C. Cells were plated on YPD agar to obtain
292 single colony isolates. One isolate was re-streaked on both selective medium and YPD. When no growth
293 was observed on selective medium the respective clone was again checked by diagnostic PCR with
294 above-mentioned primer combinations. The strain with *in vivo* assembled expression cassettes of the *E.*
295 *coli bio* genes into *ScSGA1* was stored as IMX2706.

296 ### 2.5.2 Integration of *E. coli* KAPA synthesis in IMX585 and Ethanol Red

297 Expression cassettes were PCR-amplified with the following primer pairs, thereby adding 60-bp
298 homologous sequences (Kuijpers et al., 2013b) to enable *in vivo* assembly at the *ScSGA1* locus:
299 12655/12665 for *EcfabD* (pUD978), 12656/12666 for *EcbioC* (pUD979), 12657/12667 for *EcfabB*
300 (pUD980), 12658/12668 for *EcfabG* (pUD981), 12659/12669 for *EcfabZ* (pUD982), 12660/14000 for
301 *EcfabI* (pUD983), 12455/12450 for *EcbioH* (pUD984), 14448/13718 for *EcbioF* (pUD985),
302 12663/13748 for *EcacpP* (pUD986) and 12664/12674 for *EcacpS* (pUD987). The resulting expression
303 cassettes were integrated at the *ScSGA1* locus in IMX585 and Ethanol Red, by transformation of specific

304 gRNA encoded on plasmid pUDR119 in case of IMX585 and in case of Ethanol Red by plasmid
305 pUDP145. Targeting at the *ScSGA1* locus in IMX585 was directed by strain-intrinsic Cas9 activity and
306 in Ethanol Red by expression of *Spycas9* from plasmid pUDP145 (Juergens et al., 2018). Yeast strains
307 were co-transformed with the respective plasmids and the *EcfabD, EcbioC, EcfabB, EcfabG, EcfabZ,*
308 *EcfabI, EcbioH, EcbioF, EcacpP and EcacpS* expression cassettes using the LiAc transformation
309 protocol. Transformed cells were plated on selective SMD with acetamide in case of IMX585 and on
310 YPD with hygromycin in case of Ethanol Red and incubated for 3 days at 30 °C. Genomic DNA of
311 colonies was isolated and the desired genotype confirmed by diagnostic PCR using following primer
312 combinations 11898/12761, 12762/13545, 13284/12745, 12746/12751, 12752/12759, 12760/12763,
313 12764/13281, 13280/13283, 1719/12747 and 12750/11899. Single colony isolation and plasmid
314 removal was performed as described for strain IMX2706. Strain IMX585 with *in vivo* assembled
315 expression cassettes for *E. coli* KAPA synthesis into *ScSGA1* was stocked as IMX2035 and strain
316 Ethanol Red with this modification as IMX2555 at -80 °C. The genome of strain IMX2035 was
317 sequenced by Illumina technology (Illumina, San Diego, CA) to confirm mutation-free integration of
318 the pathway genes.

319 ### 2.5.2 Gene deletion

320 To delete the native *ScBIO1* locus in *S. cerevisiae* IMX2035, it was co-transformed with plasmid
321 pUDR244 (Wronska et al., 2020) and a repair DNA fragment resulting from the annealing of oligo-
322 nucleotides 12223/12224. Transformed cells were plated on selective SMD acetamide and incubated for
323 3 days at 30 °C. Genomic DNA of colonies was isolated and the desired genotype confirmed by
324 diagnostic PCR using primer pair 7469/10873. A verified clone was inoculated in 20 mL non-selective
325 YPD for plasmid removal and incubated for 24 h at 30 °C. Cells were plated on YPD agar in order to
326 obtain single colony isolates. One isolate was re-streaked on both SMD acetamide and YPD. When no
327 growth was observed on SMD acetamide the respective clone was once again confirmed by diagnostic
328 PCR and stored as IMX2122. Similarly, to delete the heterologously expressed *EcbioF* gene, strain
329 IMX2035 was co-transformed with plasmid pUDR791 and a repair DNA fragment resulting from the
330 annealing of the oligo-nucleotides 18407/18408. After growth on selective SMD acetamide, genotyping

331 of the resulting colonies was carried out by diagnostic PCR with primer pair 1719/12747. After plasmid
332 removal a single colony was isolated and stored as IMX2707.

333 Deletion of *EcfabD*, *EcbioC* and *EcfabB* in *S. cerevisiae* IMX2555, which was derived from the diploid
334 *S. cerevisiae* strain Ethanol Red containing the KAPA synthesis pathway, was performed by
335 transformation with and integration of a deletion cassette. The transformed linear DNA fragment
336 contained 60-bp flanks homologous to the *SkADH1* promoter and the intergenic region between the
337 *EcfabB* and *EcfabG* expressional units and the KanMX expression cassette conferring resistance to
338 geneticin (Wach et al., 1994). The linear DNA fragment with the deletion cassette was obtained by PCR
339 with the primer pair 17991/17992 using plasmid pROS13 as a template. Upon homologous
340 recombination, the deletion cassette replaced one of the two copies of the three expression cassettes for
341 *EcfabD*, *EcbioC* and *EcfabB*. Electroporated cells were plated on selective YPD G418 agar plates and
342 incubated for 5 days at 30 °C. Genomic DNA of transformants was isolated and the desired genotype
343 was confirmed by diagnostic PCR using following primer combinations 11898/12761, 12762/13545,
344 13284/12745, 11898/12562, 12751/17154. The correct clone was re-streaked on YPD agar to obtain
345 single colony isolates. A single colony was once again confirmed by diagnostic PCR with above-
346 mentioned primer combinations and inoculated for stocking in 20 mL non-selective YPD. The Ethanol
347 Red strain with the integration of the KanMX cassette in the *ScSGA1* locus was stored as IMX2632.

348

349 2.6 Batch cultivation in bioreactors

350 Physiological characterization of *S. cerevisiae* IMX2122 (*Scbio1*Δ ↑*Ec*KAPA pathway) was performed
351 in anoxic bioreactors (Applikon, Delft, The Netherlands) with a working volume of 1.0 L. All cultures
352 were grown on biotin-free SMD; anoxic cultures were supplemented with sterile solutions of the
353 "anaerobic" growth factors ergosterol (10 mg L^{-1}) and Tween 80 (420 mg L^{-1}), as well as with 0.2 g L^{-1}
354 sterile antifoam C (Sigma-Aldrich). These conditions were maintained by sparging cultures with a gas
355 mixture of N_2/CO_2 (90/10 %, < 10 ppm oxygen) at a rate of 0.5 L min^{-1}. Culture pH was maintained at
356 5.0 by automatic addition of 2 M KOH. All cultures were grown at a stirrer speed of 800 rpm and at a

357 temperature of 30 °C. Oxygen diffusion in the bioreactors was minimized by using Neoprene tubing and
358 Viton O-rings, and evaporation was minimized by cooling of outlet gas to 4 °C. Oxic conditions were
359 maintained by sparging with pressurised air at a rate of 0.5 L min^{-1}. For bioreactor inocula, a 1 mL
360 aliquot of a thawed stock culture of strain IMX2122 was inoculated in 100 mL biotin-free SMD in a 500
361 mL shake flask and incubated for 20 h at 30 °C. A second 100 mL biotin-free SMD culture was started
362 by inoculating 2 mL of the first shake flask culture. Shake flasks were incubated at 30 °C and 200 rpm
363 in an Innova incubator (Brunswick Scientific). When the second culture reached mid-exponential phase
364 (OD_{660} of 3-5) it was used to inoculate the bioreactors at an OD_{660} of 0.1-0.3. Growth in the bioreactor
365 was monitored based on the CO_2 concentration in the off-gas. Specific growth rates were calculated
366 from CO_2 concentration values collected during exponential growth and covering 3-4 doublings.
367 Specific growth rate was calculated using the equation $X = X_0 e^{\mu t}$ in which μ indicates the exponential
368 growth rate. After anaerobic cultures had reached a first CO_2 production peak and the CO_2 percentage
369 in the off-gas subsequently decreased below more than 20 % of the previously measured value, a
370 computer-controlled peristaltic pump automatically removed *ca.* 90 % of the culture volume, leaving
371 *ca.* 10 % as an inoculum for the next batch cultivation cycle that occurred after refilling the reactor with
372 fresh medium. Specific growth rates in absence of oxygen were determined from the CO_2 profile after
373 two empty-refill cycles in order to deplete "anaerobic" growth factors from the pre-culturesthat were
374 run in presence of oxygen (Dekker et al., 2019).
375

376 2.7 Laboratory evolution

377 Laboratory evolution of *S. cerevisiae* IMX2122 (*Scbio1*Δ ↑*Ec*KAPA pathway) for fast anoxic growth
378 without biotin supplementation was performed in sequential-batch bioreactor cultures. Empty-refill
379 cycles in two independent anaerobic bioreactors, operated as described above, were continued until no
380 further increase of the specific growth rate was observed for at least five consecutive batch cultivation
381 cycles. Single-colony isolates from reactor A were obtained after 109 cycles and from reactor B after
382 100 cycles by plating on biotin-free SMD.

383

384 ## 2.8 Whole-genome sequence analysis

385 DNA of *S. cerevisiae* strains IMX2035, IMX2122, IMS0994 and IMS0995 grown in shake-flask
386 cultures with SMD was isolated with a Qiagen Blood & Cell Culture DNA kit (Qiagen, Germantown,
387 MD), following manufacturer's specifications. Paired-end sequencing was performed on a 350-bp PCR-
388 free insert library using an Illumina HiSeq PE150 sequencer (Novogene Company Limited, Hong
389 Kong). Sequence data was mapped to the CEN.PK113-7D genome (Salazar et al., 2017), to which the
390 sequences of the integrated expression cassettes for the heterologous genes *EcfabD, EcbioC, EcfabB,*
391 *EcfabG, EcfabZ, EcfabI, EcbioH, EcbioF, EcacpP* and *EcacpS* were manually added. Data processing
392 and chromosome copy number analysis were carried out as described previously (Bracher et al., 2017;
393 Nijkamp et al., 2012).

394

395 ## 2.9 Ploidy analysis by flow cytometry

396 For determination of ploidy, frozen aliquots of *S. cerevisiae* strains IMX2035, IMX2122 and the evolved
397 strains IMS0994 and IMS0995 were thawed and used to inoculate 20-mL cultures on SMD (IMX2035
398 and IMX2122) or on biotin-free SMD (IMS0994 and IMS0995). After incubation at 30 °C until mid-
399 exponential phase, cells were harvested, washed twice with demineralized water and stored in 70 %
400 ethanol at 4 °C. Sample preparation and staining was performed as described previously (Haase, 2004;
401 van den Broek et al., 2015). Samples were processed using a BD Accuri C6 flow cytometer (BD
402 Biosciences, San Jose, CA) and analysed using the FlowJo software package (Flowjo LLC, Ashland,
403 OR). *S. cerevisiae* strains CEN.PK113-7D and CEN.PK122 were used a haploid and diploid references,
404 respectively.

405

406 ## 2.10 Proteome analysis

407 Frozen aliquots of *S. cerevisiae* strains IMX2122 (*Scbio1*Δ ↑*Ec*KAPA pathway), IMS0994 (evolution
408 A IMX2122), and IMS0995 (evolution B IMX2122) were thawed and used to inoculate wake-up
409 cultures in 20 mL biotin-free SMD. After overnight incubation at 30 °C, these cultures were used to

410 inoculate two independent 100 mL cultures at a starting OD_{660} of 0.2. Once these cultures reached an
411 OD_{660} of 4, 1 mL was collected and centrifuged at 3000 g for 5 min, yielding a cell pellet with a volume
412 of approximately 60 µL. After protein extraction and trypsin digestion (Boonekamp et al., 2020),
413 extracted peptides were re-suspended in 30 µL of 3 % acetonitrile/0.01% trifluoroacetic acid. The
414 peptide concentration was measured using a Nanodrop spectrophotometer (Thermo Scientific) at a
415 wavelength of 280 nm. A total of 1 µg of sample was injected in a CapLC system (Thermo Scientific)
416 coupled to an Orbitrap Q-exactive HF-X mass spectrometer (Thermo Scientific). First, samples were
417 captured at a flow rate of 10 µL/min on a pre-column (µ-pre-column C18 PepMap 100, 5 µm, 100 Å)
418 and subsequently peptides were separated on a 15 cm C18 easy spray column (PepMap RSLC C18 2
419 µm, 10^4 pm, 150 µm x 15 cm) using a flow rate of 1.2 µL min^{-1}. A linear gradient from 4 % to 76 %
420 acetonitrile in water was applied over 60 min. While spraying the samples into the mass spectrometer
421 the instrument was operated in data dependent mode using settings as previously described in (Perli et
422 al., 2021). Data analysis was performed using Proteome discover 2.4 (Thermo Scientific) with fixed
423 modifications set to carbamidomethyl (C), variable modifications set to oxidation of methionine
424 residues, search mass tolerance set to 20 ppm, MS/MS tolerance set to 20 ppm, trypsin selected as
425 restriction enzyme and allowing one missed cleavage. False Discovery Rate (FDR) was set at 0.1 % and
426 the match between runs window was set to 0.7 min. Quantification was only based on unique peptides
427 and normalization between samples was based on total peptide amount. For protein search, a protein
428 database consisting of the *S. cerevisiae* S288C proteome amino-acid sequences together with the
429 sequences of the heterologously expressed proteins was used. Each strain was analyzed in independent
430 biological duplicate samples. Data processing and analysis of differentially expressed proteins was
431 conducted as previously described in (Boonekamp et al., 2020). Enrichment analysis of up- and
432 downregulated proteins in the isolates was performed using the GO Enrichment Analysis (Mi et al.,
433 2019).

434

435 # 3. Results

436 ## *3.1* Expression of the *E. coli* KAPA-biosynthesis pathway supports
437 biotin-independent growth of *S. cerevisiae* in absence of oxygen.

438 Of the currently known prokaryotic biotin-biosynthesis pathways (Figure 1), only the variant that occurs
439 in *E. coli* starts with malonyl-CoA, a key precursor for lipid synthesis in *S. cerevisiae*. To complete the
440 malonyl-CoA conversion into pimeloyl-CoA, only *EcbioC* and *EcbioH* would be required in *S.*
441 *cerevisiae* assuming that the other reactions could be performed b the native fatty acid elongation
442 machinery. We also included *EcbioF* since it is unclear whether *Sc*Bio6, the protein ortholog of *Ec*BioF,
443 can use pimeloyl-[Acp] as substrate. Integration of these three *E. coli* genes at the *SGA1* locus yielded
444 *S. cerevisiae* IMX2706. Even after prolonged oxic incubation in biotin-free synthetic medium, this
445 engineered strain did not show growth on biotin-free synthetic medium. To investigate whether this
446 inability was related to the different organization of the prokaryotic and yeast fatty-acid-synthesis
447 machineries, we introduced an additional set of expression cassettes for *E. coli* proteins involved in
448 conversion of malonyl-[Acp]-methyl ester into pimeloyl-[Acp]-methyl ester. In addition to *EcbioC, H*
449 and *F*, five genes involved in fatty-acid biosynthesis (*EcfabD, EcfabB, EcfabG, EcfabZ, EcfabI)* and
450 two genes involved in acyl carrier protein formation *(EcacpP* and *EcacpS*) were introduced. In *E. coli,*
451 the concerted action of the enzymes encoded by these genes converts malonyl-CoA into 8-amino-7-oxo-
452 nonanoate (KAPA), a metabolic intermediate of the native *S. cerevisiae* biotin pathway. Using the
453 *Spy*Cas9-expressing strain IMX585, the ten expression cassettes were integrated at the *SGA1* locus,
454 yielding *S. cerevisiae* IMX2035 (↑*Ec*KAPA pathway; Figure 2A). This engineered strain showed
455 immediate oxicgrowth on biotin-free synthetic medium, at a specific growth rate of 0.31 ± 0.01 h^{-1}.
456 Under the same conditions, the reference strain CEN.PK113-7D was unable to grow (Bracher et al.,
457 2017; Perli et al., 2020a; Wronska et al., 2020) (Figure 2B).

458 Compared to previous *S. cerevisiae* strains engineered (IMX1859, (Wronska et al., 2020) or evolved
459 (IMS0481, (Bracher et al., 2017) for biotin prototrophy, IMX2035 grew approximately 25 % slower in
460 biotin-supplemented as well as biotin-free media (Figure 2B). However, in contrast to these other biotin-
461 prototrophic strains, strain IMX2035 (↑*Ec*KAPA pathway) showed anoxic growth in biotin-free

462 medium, at specific growth rate of 0.15 ± 0.003 h^{-1}. Also in absence of oxygen, the specific growth rate
463 of strain IMX2035 on biotin-supplement medium was lower than observed in cultures of reference
464 strains (Figure 2C). These results demonstrated that expression of the *E. coli* KAPA pathway in *S.*
465 *cerevisiae* supports conversion of malonyl-CoA into KAPA and promotes biotin-independent anoxic
466 growth of *S. cerevisiae*.
467 The functionality of the *Ec*KAPA pathway in *S. cerevisiae* IMX2035 enabled us to evaluate whether the
468 orthologs *ScBIO6* and *EcbioF* are functionally redundant. To this end, *EcbioF* was deleted in strain
469 IMX2035, yielding strain IMX2707. This deletion strain did not grow on biotin-free medium, indicating
470 that the yeast 7,8-diamino-pelargonic acid aminotransferase *Sc*Bio6 cannot functionally replace the *E.*
471 *coli* 8-amino-7-oxononanoate synthase *Ec*BioF.
472

473 ## 3.2 Laboratory evolution for fast biotin-independent anoxic growth

474 To exclude the possibility that activity of the native *S. cerevisiae* biotin pathway interfered with the
475 interpretation of results, *ScBIO1* was deleted in strain IMX2035 (↑*Ec*KAPA pathway), yielding strain
476 IMX2122 (*Scbio1*Δ ↑ *Ec*KAPA pathway). *Sc*Bio1 is proposed to catalyse an as yet unidentified reaction
477 for synthesis of pimeloyl-CoA. In oxic cultures, strain IMX2122 showed similar specific growth rates
478 on biotin-supplemented and biotin-free media (specific growth rates of 0.29 ± 0.004 h^{-1} and 0.31 ± 0.003
479 h^{-1}, respectively, Figure 2B). As anticipated, strain IMX2122 grew without oxygen on biotin-free
480 medium, at a specific growth rate of 0.20 ± 0.001 h^{-1} (Figure 3C). As observed for strain IMX2035
481 (↑*Ec*KAPA pathway) biotin supplementation did not restore the specific growth rate of strain IMX2122
482 to that of reference strain CEN.PK113-7D, which in both cultivation regimes on biotin-supplemented
483 media exhibits specific growth rates of 0.32 - 0.33 h^{-1} (Bakker et al., 2001; Papapetridis et al., 2016) and
484 0.38 - 0.40 h^{-1} (van Maris et al., 2001) ,respectively.
485 To explore the evolvability of full biotin prototrophy, strain IMX2122 (*Scbio1*Δ ↑*Ec*KAPA pathway)
486 was grown in two independent, anoxic sequential batch reactors (SBRs) on biotin-free synthetic
487 medium. Throughout the course of SBR cultivation, the specific growth rate of the yeast populations in
488 the two reactions increased to close to 0.32 h^{-1}, which corresponded closely to the reported specific

489 growth rate on the congenic CEN.PK113-7D reference strain in absence of oxygen on chemically
490 defined medium with biotin (Bakker et al., 2001; Papapetridis et al., 2016) (Figure 3A, B). After 436
491 (109 batch cycles) and 400 generations (100 batch cycles) for reactor A and B, respectively, single
492 colony isolates (SCI) were obtained from each reactor (IMS0994 from reactor A and IMS0995 from
493 reactor B). Both these SCI‘s showed specific growth rates on biotin-free medium of 0.39 ± 0.01 h^{-1}.
494 Under anoxic conditions, specific growth rates of the SCI's were 0.33 ± 0.01 h^{-1} and 0.33 ± 0.02 h^{-1},
495 respectively. These specific growth rates are virtually identical to those measured in this study for the
496 reference strain CEN.PK113-7D during growth on biotin-containing synthetic medium under both
497 cultivation regimes (0.41 ± 0.01 h^{-1} and 0.31± 0.005 h^{-1}, respectively). Compared to the specific growth
498 rates of their parental strain IMX2122 on biotin-free medium in presence and absence of oxygen, those
499 of the two SCI's had increased by 34 % (p = 2E-04) and 57 % (p = 1E-04), respectively (Figure 3C).
500

501 3.3 Diploidization and subsequent copy-number reduction of *Ec*KAPA 502 biosynthesis genes contribute to evolved full biotin prototrophy

503 To identify the genetic basis of the evolved full prototrophy of the evolved isolates IMS0994 and
504 IMS0995, their genomes and that of their share parental strain IMX2122 were sequenced with Illumina
505 short-read sequencing technology and analysed. Sequence reads from the three strains were aligned with
506 a high-quality CEN.PK113-7D genome sequence (Salazar et al., 2017) supplemented with the sequence
507 of the contig comprising the expression cassettes of the engineered *E. coli* KAPA-pathway. Mapped
508 data were analysed for copy number variations (CNVs), structural modifications and single nucleotide
509 variations (SNVs) in annotated coding sequences. Prior to sequence data analysis, the nominal strain
510 ploidy of IMX2035, IMX2122, IMS0994 and IMS0995 was analysed by nucleic acid staining and
511 subsequent flow-cytometry analysis. The genetically engineered strains IMX2035 and IMX2122
512 exhibited the same ploidy as the haploid reference strain CEN.PK113-7D. In contrast, a higher
513 fluorescence intensity of both evolved SCI's (IMS0994 and IMS0995) corresponded with that of the
514 diploid reference strain CEN.PK122 (Figure 4) and indicated that a whole-genome duplication had
515 occurred in two independent evolution experiments.

516 CNV analysis of strains IMX2122 and IMS0994-5 did reveal a segmental aneuploidy of the engineered
517 SGA1 locus in which the *E. coli* KAPA pathway was integrated. As anticipated, the read coverage over
518 the contig harbouring the *E. coli* KAPA-pathway cassettes in the parental strain IMX2122 was the same
519 as that of the rest of the genome. In contrast, the evolved SCI's IMS0994 and IMS0995 showed a 50 %
520 lower coverage for a region comprising the three contiguous expression cassettes for *EcfabD*, *EcBioC*
521 and *EcfabB* (Figure 4 A-B-C). This coverage reduction relative to the rest of the genome was consistent
522 with the overall 2n ploidy of the evolved isolates (Figure 4 C-D).

523 While no homozygous SNVs were found in coding regions of the two evolved SCI's, a single
524 homozygous SNV in IMS0994 was identified in the intergenic region between *PTR2* and *MLP1* on
525 CHRXI. In addition, the two SCI's harboured a small number of heterozygous SNVs that caused amino-
526 acid changes in the peptide sequence encoded by the mutated allele. In IMS0994 nine heterozygous
527 SNVs occurring in coding sequences were found to be distributed over five genes (*FLO11*, *AGA1,*
528 MFα1, *TIF3* and *ADE3*). Similarly, IMS0995 harboured ten heterozygous SNVs scattered over the
529 coding sequences of four genes (*GLT1*, MFα1, *ECM38* and *TIF3*). Out of these heterozygous SNVs,
530 five observed in *TIF3* and one detected in MFα1 were shared by the two evolved isolates suggesting
531 that these SNVs might originate from stock cultures used to inoculate the evolution cultures. None of
532 the affected genes showed an obvious functional relationship with biotin-related cellular processes and
533 the individual impact of these SNVs was not further studied.

534 To investigate the impact of the altered gene dosage of three *E. coli* KAPA biosynthesis genes in the
535 evolved strains, levels of the *E. coli* KAPA pathway proteins were quantified in strains IMX2122,
536 IMS0994 and IMS0995. Consistent with their lower copy number relative to the remainder of the
537 genome in the evolved SCI's, abundances of the 3-oxoacyl-[Acp] synthase *Ec*FabB, the malonyl CoA-
538 acyl carrier protein transacylase *Ec*FabD and the malonyl-[Acp] O-methyltransferase *Ec*BioC in
539 IMS0994 and IMS0995 were at least 1.8-fold lower than those of the non-evolved parental strain
540 IMX2122 (Figure 5). Despite the change in ploidy, no differences in average protein abundance were
541 observed between the three strains (Figure 5A). While all expressed heterologous proteins were
542 detected, *Sc*Bio2 was the only native biotin-synthesis pathway detected in the samples.

543 Only 44 native yeast proteins in strain IMS0994 and 48 in strain IMS0995 showed a significantly
544 different abundance relative to the parental strain IMX2122, of which 22 showed a unidirectional
545 difference in the two isolates (Figures 5B and 5C). Not fewer than 20 and 26 proteins exhibited a 2-fold
546 reduction at least of their abundance in IMS0994 and IMS0995 relative to IMX2122, respectively.
547 Concomitantly, 14 and 10 proteins exhibited a 2-fold increase at least of their abundance in IMS0994
548 and IMS0995 relative to IMX2122, respectively (Figures 5B and 5C). Proteins that showed a lower level
549 in the two SCI's did not show GO-categories related to metabolic processes, whereas proteins that
550 showed a higher level in IMS0994 (^{Bonferroni}p-value = 9.98E-07) or IMS0995 (^{Bonferroni}p-value = 3.41E-
551 02) indicated an overrepresentation of proteins belonging to the GO-category 'ATP metabolic process'
552 (GO:0046034). As members of this GO category, the ATP synthase subunit Atp20 as well as the
553 cytochrome c oxidase subunits Cox5A and Cox13 showed higher levels in both isolates. In IMS0995,
554 the cytochrome c oxidase subunit Cox4 and, in IMS0994, the cytochrome b-c1 complex subunit Qcr8,
555 ATP synthase subunits Atp7 and Atp4 as well as cytochrome c oxidase subunit Cox9 also showed
556 increased levels.

557

558 3.5 Reverse engineering gene dosage of the *E. coli* KAPA biosynthesis 559 pathway contributes to improve both an- and oxic growth rate of the 560 industrial diploid strain Ethanol Red.

561 To test whether altered gene dosage of the first three genes of the oxygen-independent KAPA
562 biosynthesis pathway relative to the downstream genes, and the corresponding lower level of the
563 encoded proteins, was critical to enhance growth of engineered strains in biotin-free conditions, we
564 engineered the diploid industrial strain Ethanol Red. Using CRISPR-Cas9, which enables the
565 simultaneous modification of all gene copies in polyploid strains (Gorter de Vries et al., 2017), the ten
566 heterologous genes were introduced at the *SGA1* locus. In contrast to the parental strain Ethanol Red,
567 the resulting strain IMX2555 readily grew in biotin-free medium under oxic as well as under anoxic
568 conditions. However, in both cultivation conditions, strain IMX2555 grew slower than Ethanol Red in
569 biotin-supplemented medium (0.34 ± 0.01 h^{-1} versus 0.45 ± 0.01 h^{-1} and 0.20 ± 0.005 h^{-1} versus

570 0.42±0.001 h^{-1}, respectively; Figure 6). Specific growth rates of strain IMX2555 were not affected by
571 the presence or absence of biotin (Figure 6).

572 To reproduce the genotype observed in the evolved isolates IMS0994-5, a copy of *EcfabD, EcbioC* and
573 *EcfabB* was deleted in IMX2555 by 'pre-CRISPR' marker-assisted homologous recombination (Wach
574 et al., 1994) as it enables deletion of only one of the two copies of a targeted region in diploid strains.
575 The deletion yielded the heterozygous diploid strain IMX2632 (↑*EcfabD EcbioC EcfabB*,*G*,*Z*,*I*
576 *EcbioH*,*F EcacpP*,*S* / ↑*EcfabG,Z,I EcbioH,F EcacpP,S*). The specific growth rate of strain IMX2632
577 in anaerobic cultures on biotin-free medium was significantly higher than that of its parental strain
578 IMS2555 ($p_{\text{-value}}$ <1.0E-04; 0.30 ± 0.006 h^{-1} versus 0.19±0.004 h^{-1}). A smaller but significantly higher
579 specific growth rate ($p_{\text{-value}}$ <1.0E-04; 0.38 ± 0.007 h^{-1} versus 0.34 ± 0.003 h^{-1}) was observed in oxic
580 cultures. Despite these improvements, the engineered strain IMX2632 still grew slower than observed
581 for the Ethanol Red strain in both biotin supplemented cultures (Figure 6), suggesting additional tuning
582 of gene dosages of KAPA-pathway cassettes and/or other mutations are required for full anoxic biotin
583 prototrophy in engineered strains.

584

585 # 4. Discussion

586 The native yeast pathway for biotin biosynthesis, for which the first committed reaction remains to be
587 resolved, is oxygen dependent (Wronska et al., 2020). This study shows that functional expression of
588 the *E. coli* KAPA pathway yields *S. cerevisiae* strains that are biotin prototrophic irrespective of the
589 applied oxygen regime and whose specific growth rates can be further improved by tuning of the
590 expression levels of specific KAPA-pathway enzymes.

591 Prokaryotic biosynthesis pathways have previously been transferred between bacteria to increase biotin
592 production by bacterial hosts such as *Pseudomonas mutabilis* (Xiao et al., 2020), *Agrobacterium sp.*
593 (Shaw et al., 1999) and *E. coli* (Bali et al., 2020). For functional expression of the *E. coli* KAPA pathway
594 in *S. cerevisiae*, the different organization of prokaryotic and eukaryotic fatty-acid biosynthesis needed
595 to be considered. In the type-II FAS system of *E. coli*, individual reactions in fatty-acid synthesis are
596 catalysed by separate proteins (White et al., 2005). In contrast, the type-I FAS system of *S. cerevisiae*
597 and other fungi harbours all catalytic sites required for fatty-acid biosynthesis in domains of a large,
598 multi-functional single polypeptide or, as in *S. cerevisiae*, two polypeptides (Lomakin et al., 2007;
599 Tehlivets et al., 2007). Despite this structural difference, functional replacement of the *S. cerevisiae* type
600 I-FAS complex by the *E. coli* type-II FAS system has been demonstrated (Fernandez-Moya et al., 2015).
601 In this study, expression of only *EcbioC, H* and *F* in *S. cerevisiae* did not support biotin prototrophy.
602 This observation suggested that the yeast type-I FAS complex cannot convert malonyl-CoA methyl ester
603 into pimeloyl-[Acp] or, alternatively, that the location of the acyl-carrier function on a distinct domain
604 within a large multifunctional protein prevented *Ec*BioC from accessing its substrate. While the *S.*
605 *cerevisiae* genome additionally encodes a soluble acyl carrier protein (Acp1) and its activating enzyme
606 phosphopantetheine:protein transferase (Ppt2), these proteins participate in mitochondrial fatty-acid
607 synthesis and are located in the mitochondrial matrix (Brody et al., 1997). This localization issue was
608 circumvented by additionally expressing the *E. coli* fatty-acid synthesis genes *EcfabD*,*B*, *G*, *Z*, *I* as well
609 as *EcacpS* and *P* and, thereby, enabling cytosolic synthesis of pimeloyl-[Acp].

610 In the engineered biotin-prototrophic strain IMX2035, conversion of pimeloyl-[Acp] to 7-keto-8-
611 aminopelargonic acid (KAPA) was enabled by expression of *EcbioF*. Deletion of *EcbioF* from this strain

612 led to loss of its biotin prototrophy. Apparently, like its *B. subtilis* ortholog BioF, *S. cerevisiae* Bio6
613 cannot convert pimeloyl-[Acp] to KAPA but specifically requires pimeloyl-CoA as a substrate
614 (Manandhar and Cronan, 2018). The biotin auxotrophy of the *EcbioF* deletion strain was unlikely to be
615 caused by an insufficient expression level of Bio6 since expression of *Sc*Bio1 or *Cf*Bio1 suffices to
616 confer oxic biotin prototrophy in CEN.PK strains (Wronska et al., 2020).

617 In metabolic engineering, optimization of productivity and yield often requires balancing of the relative
618 levels of enzymes in product pathways (Naseri and Koffas, 2020). Such balancing may be especially
619 challenging when, as in the present study, the product pathway is strongly intertwined with core
620 metabolic processes of the microbial host. Optimal enzyme levels can be explored by *in vitro* (Xiao et
621 al., 2013) or *in vivo* (Lian et al., 2017; Naseri et al., 2019) approaches for combinatorial variation of the
622 amounts of relevant enzymes. Our results illustrate how adaptive laboratory evolution (Mans et al.,
623 2018; Sandberg et al., 2019), combined with access to a high-quality reference genome (Salazar et al.,
624 2017), modern sequencing technologies, proteomics and a streamlined bioinformatics pipeline
625 (Herrgard and Panagiotou, 2012; Oud et al., 2012) can provide a powerful alternative approach to gain
626 relevant information on pathway balancing.
627 Evolution of strain IMX2122 for faster biotin-independent growth involved a whole-genome duplication
628 and subsequent reduction of the copy number of three genes of the heterologous biotin-biosynthesis
629 pathway. Ploidy changes from haploid to diploid and from tetraploid to diploid have been reported in
630 previous studies on evolving yeast populations subjected to strong selection pressures such as repetitive
631 carbon-source switching (Oud et al., 2013) and ethanol stress (Voordeckers et al., 2015). A whole-
632 genome duplication was also observed after prolonged cultivation (over 1000 generations) of haploid *S.*
633 *cerevisiae* strains on complex medium (Gerstein et al., 2006). However, based on several shared
634 homozygous and heterozygous SNVs in independently evolved isolates, we cannot exclude the
635 possibility that a small subpopulation of diploid cells was already present in the predominantly haploid
636 stock cultures with which the evolution experiments were inoculated.
637 Diploidy enabled tuning of the levels of *Ec*FabD, *Ec*BioC and *Ec*FabB relative to other KAPA pathway
638 enzymes by gene deletion (Figures 4 and 5). Micro-homology-mediated end joining (MMEJ), an error-

639 prone repair mechanism that involves alignment of micro-homologous sequences before joining, is
640 typically associated with deletions and insertions that mark the original break site. In yeast, MMEJ is
641 enhanced by homologous flanking sequences of at least 12 nucleotides (Deng et al., 2014). Analysis of
642 the break-point sequence in the evolved strains revealed a 18-bp (5'-CTGGTCACTCTTTGGGTG-3')
643 direct repeat in *EcfabD* (positions 265-283) and in *EcfabB* (positions 991 and 1009) that perfectly
644 flanked the heterozygous deletion. This observation strongly suggests that MMEJ was responsible for
645 the deletion (Seol et al., 2018). Deliberate introduction of short direct repeats in between clustered
646 expression cassettes introduced into diploid or tetraploid strains by Cas9-medidated integration,
647 followed by adaptive laboratory evolution, may be an attractive approach for exploring optimal gene
648 dosages in heterologously expressed pathways whose *in vivo* activity can be coupled to growth or
649 survival.
650 Deletion of a copy of *EcfabB, D* and *EcbioC* in the evolved diploid strains is likely to have mitigated a
651 too strong competition for malonyl-CoA between the heterologously expressed KAPA pathway and
652 native fatty-acid synthesis. This interpretation is consistent with the observed sub-optimal growth of the
653 non-evolved parental strain on biotin-supplemented medium. The relevance of the segmental aneuploidy
654 in the evolved strains was demonstrated by its reconstruction in the diploid industrial *S. cerevisiae* strain
655 Ethanol Red. The anoxic specific growth rate of the thus engineered biotin-prototrophic strain was *ca.*
656 25 % lower than that of biotin-supplemented cultures of non-engineered Ethanol Red. Although further
657 targeted engineering and/or laboratory evolution is required for industrial implementation, our results
658 demonstrate the feasibility of introducing anoxicbiotin prototrophy into industrial *S. cerevisiae* strains.
659 Growth of wild-type *S. cerevisiae* strains on chemically defined media in absence of oxygen depends
660 on supplementation of several nutrients, including ergosterol (Andreasen, 1953), nicotinic acid (Panozzo
661 et al., 2002), pantothenate (Perli et al., 2020b) and biotin (Wronska et al., 2020). Although essential for
662 fast growth, the unsaturated fatty acid requirement of *S. cerevisiae* for anoxic growth is not absolute (da
663 Costa et al., 2018; Dekker et al., 2019). Several metabolic strategies have recently been studied to
664 eliminate these biosynthetic oxygen requirements. Expression of a squalene-tetrahymanol cyclase gene
665 from *Tetrahymena thermophila* was shown to enable synthesis of the sterol surrogate tetrahymanol and
666 anoxic growth of *S. cerevisiae* in sterol-free media (Wiersma et al., 2020). Similarly, expression of

667 fungal genes encoding an L-aspartate oxidase (NadB) and a quinolinate synthase (NadA) enabled
668 nicotinic acid prototrophy without oxygen, while expression of heterologous L-aspartate-
669 decarboxylases (AdcA) supported anoxic growth in the absence of pantothenate (Perli et al., 2020b). In
670 terms of anoxic synthesis of cofactors, this leaves the puzzling case of thiamine, whose synthesis by
671 yeast has been reported to be oxygen-dependent although the enzymes involved do not appear to require
672 molecular oxygen (Wightman and Meacock, 2003). Further research on engineering anoxic cofactor
673 synthesis in yeast is therefore not only relevant for the development of robust, prototrophic and
674 feedstock-agnostic yeast strains for application in anoxic processes, but also for fundamental
675 understanding of native biosynthetic pathways.

676

677 # 5. Conclusions

678 Functional expression of ten *E. coli* enzymes involved in KAPA synthesis enabled biotin-prototrophic
679 growth of *S. cerevisiae* irrespective of oxygen supply. Adaptive laboratory evolution, genome
680 resequencing, proteomics and reverse engineering of observed copy-number differences in a naive strain
681 identified balancing of the relative levels of KAPA pathway enzymes as a key requirement for fast
682 biotin-prototrophic growth. This metabolic engineering strategy can be used to construct *S. cerevisiae*
683 cell factories for anaerobic bioprocesses based on feedstocks with low or variable biotin contents.

684 # 6. Data availability

685 The genome sequencing data of the *S. cerevisiae* strains IMX2035, IMX2122, IMS0994 and IMS0995
686 can be found in the NCBI archive BioProject under the accession number PRJNA717156. The codon
687 optimised sequences of the heterologous genes used in this study and the raw data used to draw graphs
688 on Figures 2, 3, 5 and 6 are available at the 4TU.Centre for research data repository
689 (https://researchdata.4tu.nl/) under the https://doi.org/10.4121/14308007.

690

Acknowledgments

We thank Pilar de la Torre Cortés for whole genome sequencing, Marijke Luttik for guidance during ploidy analysis, Jonna Bouwknegt, Sanne Wiersma and Wijb Dekker for instructions on anaerobic chamber experiments. We thank Tune Wulff from DTU Biosustain for the proteomics analysis. A.K.W., J.-M.G.D., and J.T.P. designed experiments. A.K.W. performed all experiments, except the proteome samples, which were prepared by T.P. E.A.F.D.H provided experimental support and valuable input on the design of bioreactor experiments. M.V.D.B. developed methods and wrote scripts for whole genome sequence and proteome analysis. A.K.W., J.-M.G.D. and J.T.P. wrote the manuscript. All authors read and commented on the manuscript and approved the final version. A.K.W., J.-M.G.D., and J.T.P. are inventors on a patent application (WO2020234215 (A1)) related to this work. The remaining authors have no competing interests to declare.

Funding

A.K.W., T.P. and J.-M.G.D. were supported by the European Union's Horizon 2020 research and innovation program under the Marie Skłodowska-Curie action PAcMEN (grant agreement no. 722287). J.T.P. is funded by an Advanced Grant of the European Research Council (grant no. 694633).

References

Agarwal, V., Lin, S., Lukk, T., Nair, S. K., Cronan, J. E., 2012. Structure of the enzyme-acyl carrier protein (ACP) substrate gatekeeper complex required for biotin synthesis. Proc Natl Acad Sci U S A. 109, 17406-11.

Alfenore, S., Molina-Jouve, C., Guillouet, S. E., Uribelarrea, J. L., Goma, G., Benbadis, L., 2002. Improving ethanol production and viability of *Saccharomyces cerevisiae* by a vitamin feeding strategy during fed-batch process. Appl Microbiol Biotechnol. 60, 67-72.

Andreasen, A. A. S., T. J., 1953. Anaerobic nutrition of *Saccharomyces cerevisiae*. I. Ergosterol requirement for growth in a defined medium. J Cell Physiol. 41, 23–36.

Bakker, B. M., Overkamp, K. M., van Maris, A. J., Kotter, P., Luttik, M. A., van Dijken, J. P., Pronk, J. T., 2001. Stoichiometry and compartmentation of NADH metabolism in *Saccharomyces cerevisiae*. FEMS Microbiol Rev. 25, 15-37.

Bali, A. P., Lennox-Hvenekilde, D., Myling-Petersen, N., Buerger, J., Salomonsen, B., Gronenberg, L. S., Sommer, M. O. A., Genee, H. J., 2020. Improved biotin, thiamine, and lipoic acid biosynthesis by engineering the global regulator IscR. Metab Eng. 60, 97-109.

Basso, L. C., de Amorim, H. V., de Oliveira, A. J., Lopes, M. L., 2008. Yeast selection for fuel ethanol production in Brazil. FEMS Yeast Res. 8, 1155-63.

Bohlscheid, J. C., Fellman, J. K., Wang, X. D., Ansen, D., Edwards, C. G., 2007. The influence of nitrogen and biotin interactions on the performance of *Saccharomyces* in alcoholic fermentations. J Appl Microbiol. 102, 390-400.

Boonekamp, F. J., Dashko, S., Duiker, D., Gehrmann, T., van den Broek, M., den Ridder, M., Pabst, M., Robert, V., Abeel, T., Postma, E. D., Daran, J. M., Daran-Lapujade, P., 2020. Design and Experimental Evaluation of a Minimal, Innocuous Watermarking Strategy to Distinguish Near-Identical DNA and RNA Sequences. Acs Synth Biol. 9, 1361-1375.

Bower, S., Perkins, J. B., Yocum, R. R., Howitt, C. L., Rahaim, P., Pero, J., 1996. Cloning, sequencing, and characterization of the *Bacillus subtilis* biotin biosynthetic operon. J Bacteriol. 178, 4122-30.

Bracher, J. M., de Hulster, E., Koster, C. C., van den Broek, M., Daran, J. G., van Maris, A. J. A., Pronk, J. T., 2017. Laboratory Evolution of a Biotin-Requiring *Saccharomyces cerevisiae* Strain for Full Biotin Prototrophy and Identification of Causal Mutations. Appl Environ Microbiol. 83, AEM.00892-17.

Brandberg, T., Karimi, K., Taherzadeh, M. J., Franzen, C. J., Gustafsson, L., 2007. Continuous fermentation of wheat-supplemented lignocellulose hydrolysate with different types of cell retention. Biotechnol Bioeng. 98, 80-90.

Brandberg, T., Sanandaji, N., Gustafsson, L., Franzen, C. J., 2005. Continuous fermentation of undetoxified dilute acid lignocellulose hydrolysate by *Saccharomyces cerevisiae* ATCC 96581 using cell recirculation. Biotechnol Prog. 21, 1093-101.

Brody, S., Oh, C., Hoja, U., Schweizer, E., 1997. Mitochondrial acyl carrier protein is involved in lipoic acid synthesis in *Saccharomyces cerevisiae*. FEBS Lett. 408, 217-20.

Brown, G. B., Du Vigneaud, V., 1941. The effect of certain reagents on the activity of biotin. J Biol Chem. 141, 85–89.

da Costa, B. L. V., Basso, T. O., Raghavendran, V., Gombert, A. K., 2018. Anaerobiosis revisited: growth of *Saccharomyces cerevisiae* under extremely low oxygen availability. Appl Microbiol Biotechnol. 102, 2101-2116.

Dekker, W. J. C., Wiersma, S. J., Bouwknegt, J., Mooiman, C., Pronk, J. T., 2019. Anaerobic growth of *Saccharomyces cerevisiae* CEN.PK113-7D does not depend on synthesis or supplementation of unsaturated fatty acids. FEMS Yeast Res. 19, foz060.

Deng, S. K., Gibb, B., de Almeida, M. J., Greene, E. C., Symington, L. S., 2014. RPA antagonizes microhomology-mediated repair of DNA double-strand breaks. Nat Struct Mol Biol. 21, 405-12.

Entian, K. D., Kotter, P., 2007. Yeast genetic strain and plasmid collections. Method Microbiol. 36, 629-666.

Fernandez-Moya, R., Leber, C., Cardenas, J., Da Silva, N. A., 2015. Functional replacement of the *Saccharomyces cerevisiae* fatty acid synthase with a bacterial type II system allows flexible product profiles. Biotechnol Bioeng. 112, 2618-23.

Gerstein, A. C., Chun, H. J., Grant, A., Otto, S. P., 2006. Genomic convergence toward diploidy in *Saccharomyces cerevisiae*. PLoS Genet. 2, e145.

Gietz, R. D., Woods, R. A., 2002. Transformation of yeast by lithium acetate/single-stranded carrier DNA/polyethylene glycol method. Method Enzymol. 350, 87-96.

Gorter de Vries, A. R., de Groot, P. A., van den Broek, M., Daran, J. G., 2017. CRISPR-Cas9 mediated gene deletions in lager yeast *Saccharomyces pastorianus*. Microb Cell Fact. 16, 222.

Grote, A., Hiller, K., Scheer, M., Munch, R., Nortemann, B., Hempel, D. C., Jahn, D., 2005. JCat: a novel tool to adapt codon usage of a target gene to its potential expression host. Nucleic Acids Res. 33, W526-31.

Haase, S. B., 2004. Cell cycle analysis of budding yeast using SYTOX Green. Curr Protoc Cytom. Chapter 7, Unit 7 23.

Hahn-Hagerdal, B., Karhumaa, K., Larsson, C. U., Gorwa-Grauslund, M., Gorgens, J., van Zyl, W. H., 2005. Role of cultivation media in the development of yeast strains for large scale industrial use. Microb Cell Fact. 4, 31.

Hall, C., Dietrich, F. S., 2007. The reacquisition of biotin prototrophy in *Saccharomyces cerevisiae* involved horizontal gene transfer, gene duplication and gene clustering. Genetics. 177, 2293-307.

Hassing, E. J., de Groot, P. A., Marquenie, V. R., Pronk, J. T., Daran, J. G., 2019. Connecting central carbon and aromatic amino acid metabolisms to improve de novo 2-phenylethanol production in *Saccharomyces cerevisiae*. Metab Eng. 56, 165-180.

Herrgard, M., Panagiotou, G., 2012. Analyzing the genomic variation of microbial cell factories in the era of "New Biotechnology". Comput Struct Biotechnol J. 3, e201210012.

Inoue, H., Nojima, H., Okayama, H., 1990. High efficiency transformation of *Escherichia coli* with plasmids. Gene. 96, 23-8.

Jackson, W. R., Macek, T. J., 1944. B Complex Vitamins in Sugar Cane and Sugar Cane Juice. Ind Eng Chem. 36, 261-263.

Juergens, H., Varela, J. A., Gorter de Vries, A. R., Perli, T., Gast, V. J. M., Gyurchev, N. Y., Rajkumar, A. S., Mans, R., Pronk, J. T., Morrissey, J. P., Daran, J. G., 2018. Genome editing in *Kluyveromyces* and *Ogataea* yeasts using a broad-host-range Cas9/gRNA co-expression plasmid. FEMS Yeast Res. 18.

Kuijpers, N. G., Chroumpi, S., Vos, T., Solis-Escalante, D., Bosman, L., Pronk, J. T., Daran, J. M., Daran-Lapujade, P., 2013a. One-step assembly and targeted integration of multigene constructs assisted by the I-SceI meganuclease in *Saccharomyces cerevisiae*. FEMS Yeast Res. 13, 769-81.

Kuijpers, N. G., Solis-Escalante, D., Bosman, L., van den Broek, M., Pronk, J. T., Daran, J. M., Daran-Lapujade, P., 2013b. A versatile, efficient strategy for assembly of multi-fragment expression vectors in *Saccharomyces cerevisia*e using 60 bp synthetic recombination sequences. Microb Cell Fact. 12, 47.

Lee, M. E., DeLoache, W. C., Cervantes, B., Dueber, J. E., 2015. A highly characterized yeast toolkit for modular, multipart assembly. Acs Synth Biol. 4, 975-986.

Lian, J., HamediRad, M., Hu, S., Zhao, H., 2017. Combinatorial metabolic engineering using an orthogonal tri-functional CRISPR system. Nat Commun. 8, 1688.

Lin, S., Cronan, J. E., 2012. The BioC O-methyltransferase catalyzes methyl esterification of malonyl-acyl carrier protein, an essential step in biotin synthesis. J Biol Chem. 287, 37010-20.

Lin, S., Hanson, R. E., Cronan, J. E., 2010. Biotin synthesis begins by hijacking the fatty acid synthetic pathway. Nat Chem Biol. 6, 682-8.

Lomakin, I. B., Xiong, Y., Steitz, T. A., 2007. The crystal structure of yeast fatty acid synthase, a cellular machine with eight active sites working together. Cell. 129, 319-32.

Looke, M., Kristjuhan, K., Kristjuhan, A., 2011. Extraction of genomic DNA from yeasts for PCR-based applications. Biotechniques. 50**,** 325-.

Manandhar, M., Cronan, J. E., 2017. Pimelic acid, the first precursor of the *Bacillus subtilis* biotin synthesis pathway, exists as the free acid and is assembled by fatty acid synthesis. Mol Microbiol. 104**,** 595-607.

Manandhar, M., Cronan, J. E., 2018. A Canonical Biotin Synthesis Enzyme, 8-Amino-7-Oxononanoate Synthase (BioF), Utilizes Different Acyl Chain Donors in *Bacillus subtilis* and *Escherichia coli*. Appl Environ Microbiol. 84.

Mans, R., Daran, J. G., Pronk, J. T., 2018. Under pressure: evolutionary engineering of yeast strains for improved performance in fuels and chemicals production. Curr Opin Biotechnol. 50**,** 47-56.

Mans, R., van Rossum, H. M., Wijsman, M., Backx, A., Kuijpers, N. G., van den Broek, M., Daran-Lapujade, P., Pronk, J. T., van Maris, A. J., Daran, J. M., 2015. CRISPR/Cas9: a molecular Swiss army knife for simultaneous introduction of multiple genetic modifications in *Saccharomyces cerevisiae*. FEMS Yeast Res. 15**,** fov004.

Mauri, L. M., Alzamora, S. M., Chirife, J., Tomio, M. J., 1989. Review: Kinetic parameters for thiamine degradation in foods and model solutions of high water activity. International Journal of Food Science & Technology. 24**,** 1-9.

Medina, K., Boido, E., Dellacassa, E., Carrau, F., 2012. Growth of non-*Saccharomyces* yeasts affects nutrient availability for *Saccharomyces cerevisiae* during wine fermentation. Int J Food Microbiol. 157**,** 245-50.

Mi, H., Muruganujan, A., Ebert, D., Huang, X., Thomas, P. D., 2019. PANTHER version 14: more genomes, a new PANTHER GO-slim and improvements in enrichment analysis tools. Nucleic Acids Res. 47**,** D419-D426.

Naseri, G., Behrend, J., Rieper, L., Mueller-Roeber, B., 2019. COMPASS for rapid combinatorial optimization of biochemical pathways based on artificial transcription factors. Nat Commun. 10**,** 2615.

Naseri, G., Koffas, M. A. G., 2020. Application of combinatorial optimization strategies in synthetic biology. Nat Commun. 11**,** 2446.

Nijkamp, J. F., van den Broek, M. A., Geertman, J. M., Reinders, M. J., Daran, J. M., de Ridder, D., 2012. *De novo* detection of copy number variation by co-assembly. Bioinformatics. 28**,** 3195-202.

Otsuka, A. J., Buoncristiani, M. R., Howard, P. K., Flamm, J., Johnson, C., Yamamoto, R., Uchida, K., Cook, C., Ruppert, J., Matsuzaki, J., 1988. The *Escherichia coli* biotin biosynthetic enzyme sequences predicted from the nucleotide sequence of the bio operon. J Biol Chem. 263**,** 19577-85.

Oud, B., Guadalupe-Medina, V., Nijkamp, J. F., de Ridder, D., Pronk, J. T., van Maris, A. J., Daran, J. M., 2013. Genome duplication and mutations in *ACE2* cause multicellular, fast-sedimenting phenotypes in evolved *Saccharomyces cerevisiae*. Proc Natl Acad Sci U S A. 110**,** E4223-31.

Oud, B., van Maris, A. J., Daran, J. M., Pronk, J. T., 2012. Genome-wide analytical approaches for reverse metabolic engineering of industrially relevant phenotypes in yeast. FEMS Yeast Res. 12**,** 183-96.

Panozzo, C., Nawara, M., Suski, C., Kucharczyka, R., Skoneczny, M., Becam, A. M., Rytka, J., Herbert, C. J., 2002. Aerobic and anaerobic NAD^+ metabolism in *Saccharomyces cerevisiae*. FEBS Lett. 517**,** 97-102.

Papapetridis, I., Goudriaan, M., Vazquez Vitali, M., de Keijzer, N. A., van den Broek, M., van Maris, A. J. A., Pronk, J. T., 2018. Optimizing anaerobic growth rate and fermentation kinetics in *Saccharomyces cerevisiae* strains expressing Calvin-cycle enzymes for improved ethanol yield. Biotechnol Biofuels. 11**,** 17.

Papapetridis, I., van Dijk, M., Dobbe, A. P., Metz, B., Pronk, J. T., van Maris, A. J., 2016. Improving ethanol yield in acetate-reducing *Saccharomyces cerevisiae* by cofactor engineering of 6-phosphogluconate dehydrogenase and deletion of *ALD6*. Microb Cell Fact. 15**,** 67.

Patton, D. A., Schetter, A. L., Franzmann, L. H., Nelson, K., Ward, E. R., Meinke, D. W., 1998. An embryo-defective mutant of *Arabidopsis* disrupted in the final step of biotin synthesis. Plant Physiol. 116**,** 935-46.

Pejin, D., DoŠEnoviĆ, I., Razmovski, R., KaradŽIĆ, V., GrbiĆ, J., 1996. Dependence of biotin content on molasses composition. J Food Qual. 19**,** 353-361.

Perli, T., Moonen, D. P. I., van den Broek, M., Pronk, J. T., Daran, J. M., 2020a. Adaptive Laboratory Evolution and Reverse Engineering of Single-Vitamin Prototrophies in *Saccharomyces cerevisiae*. Appl Environ Microbiol. 86.

Perli, T., van der Vorm, D. N. A., Wassink, M., van den Broek, M., Pronk, J. T., Daran, J. M., 2021. Engineering heterologous molybdenum-cofactor-biosynthesis and nitrate-assimilation pathways enables nitrate utilization by *Saccharomyces cerevisiae*. Metab Eng. 65**,** 11-29.

Perli, T., Vos, A. M., J., B., Dekker, W. J. C., Wiersma, S. J., Mooiman, C., Ortiz-Merino, R. A., Daran, J.-M. G., Pronk, J. T., 2020b. Identification of oxygen-independent pathways for pyridine-nucleotide and Coenzyme-A synthesis in anaerobic fungi by expression of candidate genes in yeast. bioRxiv. 2020.07.06.189415**,** doi: https://doi.org/10.1101/2020.07.06.189415.

Perli, T., Wronska, A. K., Ortiz-Merino, R. A., Pronk, J. T., Daran, J. M., 2020c. Vitamin requirements and biosynthesis in *Saccharomyces cerevisiae*. Yeast. 37**,** 283-304.

Saidi, B., Warthesen, J. J., 1983. Influence of pH and light on the kinetics of vitamin B_6 degradation. J Agric Food Chem. 31**,** 876-880.

Sakaki, K., Ohishi, K., Shimizu, T., Kobayashi, I., Mori, N., Matsuda, K., Tomita, T., Watanabe, H., Tanaka, K., Kuzuyama, T., Nishiyama, M., 2020. A suicide enzyme catalyzes multiple reactions for biotin biosynthesis in Cyanobacteria. Nat Chem Biol. 16**,** 415-422.

Salazar, A. N., Gorter de Vries, A. R., van den Broek, M., Wijsman, M., de la Torre Cortes, P., Brickwedde, A., Brouwers, N., Daran, J. G., Abeel, T., 2017. Nanopore sequencing enables near-complete *de novo* assembly of *Saccharomyces cerevisiae* reference strain CEN.PK113-7D. FEMS Yeast Res. 17**,** fox074.

Sandberg, T. E., Salazar, M. J., Weng, L. L., Palsson, B. O., Feist, A. M., 2019. The emergence of adaptive laboratory evolution as an efficient tool for biological discovery and industrial biotechnology. Metab Eng. 56**,** 1-16.

Schnellbaecher, A., Binder, D., Bellmaine, S., Zimmer, A., 2019. Vitamins in cell culture media: Stability and stabilization strategies. Biotechnol Bioeng. 116**,** 1537-1555.

Seol, J. H., Shim, E. Y., Lee, S. E., 2018. Microhomology-mediated end joining: Good, bad and ugly. Mutat Res. 809**,** 81-87.

Shaw, N., Lehner, B., Fuhrmann, M., Kulla, H., Brass, J., Birch, O., Tinschert, A., Venetz, D., Venetz, V. V., Sanchez, J. C., Tonella, L., Hochstrasser, D., 1999. Biotin production under limiting growth conditions by *Agrobacterium/Rhizobium* HK4 transformed with a modified *Escherichia coli bio* operon. J Ind Microbiol Biotechnol. 22**,** 590-599.

Solis-Escalante, D., Kuijpers, N. G., Bongaerts, N., Bolat, I., Bosman, L., Pronk, J. T., Daran, J. M., Daran-Lapujade, P., 2013. amdSYM, a new dominant recyclable marker cassette for Saccharomyces cerevisiae. FEMS Yeast Res. 13**,** 126-39.

Stok, J. E., De Voss, J., 2000. Expression, purification, and characterization of BioI: a carbon-carbon bond cleaving cytochrome P450 involved in biotin biosynthesis in *Bacillus subtilis*. Arch Biochem Biophys. 384**,** 351-60.

Streit, W. R., Entcheva, P., 2003. Biotin in microbes, the genes involved in its biosynthesis, its biochemical role and perspectives for biotechnological production. Appl Microbiol Biotechnol. 61**,** 21-31.

Tehlivets, O., Scheuringer, K., Kohlwein, S. D., 2007. Fatty acid synthesis and elongation in yeast. Biochim Biophys Acta. 1771**,** 255-70.

van den Broek, M., Bolat, I., Nijkamp, J. F., Ramos, E., Luttik, M. A., Koopman, F., Geertman, J. M., de Ridder, D., Pronk, J. T., Daran, J. M., 2015. Chromosomal Copy Number Variation in *Saccharomyces pastorianus* Is Evidence for Extensive Genome Dynamics in Industrial Lager Brewing Strains. Appl Environ Microbiol. 81**,** 6253-67.

910 van Dijk, M., Mierke, F., Nygard, Y., Olsson, L., 2020. Nutrient-supplemented propagation of
911 *Saccharomyces cerevisiae* improves its lignocellulose fermentation ability. AMB Express. 10**,**
912 157.
913 van Maris, A. J., Bakker, B. M., Brandt, M., Boorsma, A., Teixeira de Mattos, M. J., Grivell, L. A., Pronk,
914 J. T., Blom, J., 2001. Modulating the distribution of fluxes among respiration and fermentation
915 by overexpression of *HAP4* in *Saccharomyces cerevisiae*. FEMS Yeast Res. 1**,** 139-49.
916 Verduyn, C., Postma, E., Scheffers, W. A., Van Dijken, J. P., 1992. Effect of benzoic acid on metabolic
917 fluxes in yeasts: a continuous-culture study on the regulation of respiration and alcoholic
918 fermentation. Yeast. 8**,** 501-17.
919 Voordeckers, K., Kominek, J., Das, A., Espinosa-Cantu, A., De Maeyer, D., Arslan, A., Van Pee, M., van
920 der Zande, E., Meert, W., Yang, Y., Zhu, B., Marchal, K., DeLuna, A., Van Noort, V., Jelier, R.,
921 Verstrepen, K. J., 2015. Adaptation to High Ethanol Reveals Complex Evolutionary Pathways.
922 PLoS Genet. 11**,** e1005635.
923 Wach, A., Brachat, A., Pohlmann, R., Philippsen, P., 1994. New heterologous modules for classical or
924 PCR-based gene disruptions in *Saccharomyces cerevisiae*. Yeast. 10**,** 1793-808.
925 White, S. W., Zheng, J., Zhang, Y. M., Rock, 2005. The structural biology of type II fatty acid biosynthesis.
926 Annu Rev Biochem. 74**,** 791-831.
927 Wiersma, S. J., Mooiman, C., Giera, M., Pronk, J. T., 2020. Squalene-Tetrahymanol Cyclase Expression
928 Enables Sterol-Independent Growth of *Saccharomyces cerevisiae*. Appl Environ Microbiol. 86.
929 Wightman, R., Meacock, P. A., 2003. The *THI5* gene family of *Saccharomyces cerevisiae:* distribution of
930 homologues among the hemiascomycetes and functional redundancy in the aerobic
931 biosynthesis of thiamin from pyridoxine. Microbiology (Reading). 149**,** 1447-1460.
932 Wronska, A. K., Haak, M. P., Geraats, E., Bruins Slot, E., van den Broek, M., Pronk, J. T., Daran, J. M.,
933 2020. Exploiting the Diversity of Saccharomycotina Yeasts To Engineer Biotin-Independent
934 Growth of *Saccharomyces cerevisiae*. Appl Environ Microbiol. 86**,** AEM.00270-20.
935 Xiao, F., Wang, H., Shi, Z., Huang, Q., Huang, L., Lian, J., Cai, J., Xu, Z., 2020. Multi-level metabolic
936 engineering of *Pseudomonas mutabilis* ATCC31014 for efficient production of biotin. Metab
937 Eng. 61**,** 406-415.
938 Xiao, X., Yu, X., Khosla, C., 2013. Metabolic flux between unsaturated and saturated fatty acids is
939 controlled by the FabA:FabB ratio in the fully reconstituted fatty acid biosynthetic pathway of
940 *Escherichia coli*. Biochemistry. 52**,** 8304-12.

941

Tables

Table 1 | List of strains constructed and used in this study.

Strain	Genotype	Reference or source
CEN.PK113-7D	*MAT*a *MAL2-8c SUC2*	(Entian and Kotter, 2007)
CEN.PK-122	*MAT*a/*MATα*	(Entian and Kotter, 2007)
IMS0481	Single colony isolate of CEN.PK113-7D evolved in synthetic medium without biotin	(Bracher et al., 2017)
IMX1859	*MAT*a *can1*Δ::*cas9-natNT2 Scsga1*Δ::*ScPYK1*p-*CfBIO1-ScBIO1*t	(Wronska et al., 2020)
IMX585	*MAT*a *can1*Δ::*cas9-natNT2*	(Mans et al., 2015)
IMX2600	*MAT*a *can1*Δ::*cas9-natNT2*	This study
IMX2035	*MAT*a *can1*Δ::*cas9-natNT2 Scsga1*Δ::*SkADH1*p-*EcfabD-ScADH1*t_*SkTDH2*p-*EcbioC-ScTEF2*t_*SkPDC1*p-*EcfabB-ScPYK1*t_*SkFBA1*p-*EcfabG-ScFBA1*t_*SePDC1*p-*EcfabZ-ScPDC1*t_*ScENO2*p-*EcfabI-ScPFK2*t_*ScPYK1*p-*EcbioH-ScPGI1*t_*ScPFK2*p-*EcbioF-ScTPI*t_*ScPGI1*p-*EcacpP-ScGPM1*t_*ScHXK2*p-*EcacpS-ScTDH3*t	This study
IMX2122	*MAT*a *can1*Δ::*cas9-natNT2 Scsga1*Δ::*SkADH1*p-*EcfabD-ScADH1*t_*SkTDH2*p-*EcbioC-ScTEF2*t_*SkPDC1*p-*EcfabB-ScPYK1*t_*SkFBA1*p-*EcfabG-ScFBA1*t_*SePDC1*p-*EcfabZ-ScPDC1*t_*ScENO2*p-*EcfabI-ScPFK2*t_*ScPYK1*p-*EcbioH-ScPGI1*t_*ScPFK2*p-*EcbioF-ScTPI*t_*ScPGI1*p-*EcacpP-ScGPM1*t_*ScHXK2*p-*EcacpS-ScTDH3*t *Scbio1*Δ	This study
IMS0994	Single colony isolate of IMX2122 evolved under anoxic conditions without biotin in bioreactor A	This study
IMS0995	Single colony isolate of IMX2122 evolved under anoxic conditions without biotin in bioreactor B	This study
Ethanol Red	*MAT*a/α (diploid prototrophic industrial bioethanol production strain)	F.R. Lesaffre
IMX2555	Ethanol Red *Scsga1*Δ::*SkADH1*p-*EcfabD-ScADH1*t_*SkTDH2*p-*EcbioC-ScTEF2*t_*SkPDC1*p-*EcfabB-ScPYK1*t_*SkFBA1*p-*EcfabG-ScFBA1*t_*SePDC1*p-*EcfabZ-ScPDC1*t_*ScENO2*p-*EcfabI-ScPFK2*t_*ScPYK1*p-*EcbioH-ScPGI1*t_*ScPFK2*p-*EcbioF-ScTPI*t_*ScPGI1*p-*EcacpP-ScGPM1*t_*ScHXK2*p-*EcacpS-ScTDH3*t/*Scsga1*Δ::*SkADH1*p-*EcfabD-ScADH1*t_*SkTDH2*p-*EcbioC-ScTEF2*t_*SkPDC1*p-*EcfabB-ScPYK1*t_*SkFBA1*p-*EcfabG-ScFBA1*t_*SePDC1*p-*EcfabZ-ScPDC1*t_*ScENO2*p-*EcfabI-ScPFK2*t_*ScPYK1*p-*EcbioH-ScPGI1*t_*ScPFK2*p-*EcbioF-ScTPI*t_*ScPGI1*p-*EcacpP-ScGPM1*t_*ScHXK2*p-*EcacpS-ScTDH3*t	This study
IMX2632	Ethanol Red *Scsga1*Δ::*SkADH1*p-*EcfabD-ScADH1*t_*SkTDH2*p-*EcbioC-ScTEF2*t_*SkPDC1*p-*EcfabB-ScPYK1*t_*SkFBA1*p-*EcfabG-ScFBA1*t_*SePDC1*p-*EcfabZ-ScPDC1*t_*ScENO2*p-*EcfabI-ScPFK2*t_*ScPYK1*p-*EcbioH-ScPGI1*t_*ScPFK2*p-*EcbioF-ScTPI*t_*ScPGI1*p-*EcacpP-ScGPM1*t_*ScHXK2*p-*EcacpS-ScTDH3*t/*Scsga1*Δ::*AgTEF*p-kanMX-*AgTEF*t_*SkFBA1*p-*EcfabG-ScFBA1*t_*SePDC1*p-*EcfabZ-ScPDC1*t_*ScENO2*p-*EcfabI-ScPFK2*t_*ScPYK1*p-*EcbioH-ScPGI1*t_*ScPFK2*p-*EcbioF-ScTPI*t_*ScPGI1*p-*EcacpP-ScGPM1*t_*ScHXK2*p-*EcacpS-ScTDH3*t	This study
IMX2706	*MAT*a *can1*Δ::*cas9-natNT2 Scsga1*Δ::*SkTDH2*p-*EcbioC-ScTEF2*t_*ScPYK1*p-*EcbioH-ScPGI1*t_*ScPFK2*p-*EcbioF*Δ-*ScTPI*t	This study
IMX2707	*MAT*a *can1*Δ::*cas9-natNT2 Scsga1*Δ::*SkADH1*p-*EcfabD-ScADH1*t_*SkTDH2*p-*EcbioC-ScTEF2*t_*SkPDC1*p-*EcfabB-ScPYK1*t_*SkFBA1*p-*EcfabG-ScFBA1*t_*SePDC1*p-*EcfabZ-ScPDC1*t_*ScENO2*p-*EcfabI-ScPFK2*t_*ScPYK1*p-*EcbioH-ScPGI1*t_*ScPFK2*p-*EcbioF*Δ-*ScTPI*t_*ScPGI1*p-*EcacpP-ScGPM1*t_*ScHXK2*p-*EcacpS-ScTDH3*t	This study

945 Table 2 | List of plasmids constructed and used in this study.

Name	Characteristics	Reference or source
pGGkd015	*bla* ColE1 Gfp dropout	(Hassing et al., 2019)
pGGkp028	*cat* ColE1 *ScENO2*p	(Hassing et al., 2019)
pGGkp031	*cat* ColE1 *ScPFK2*p	This study
pGGkp033	*cat* ColE1 *ScPGI1*p	(Hassing et al., 2019)
pGGkp037	*cat* ColE1 *ScADH1*t	(Hassing et al., 2019)
pGGkp038	*cat* ColE1*ScTEF2*t	(Hassing et al., 2019)
pGGkp040	*cat* ColE1 *ScPYK1*t	(Hassing et al., 2019)
pGGkp041	*cat* ColE1 *ScTDH3*t	(Hassing et al., 2019)
pGGkp042	*cat* ColE1 *ScTPI*t	This study
pGGkp044	*cat* ColE1 *ScPGI1*t	This study
pGGkp045	*cat* ColE1 *ScPDC1*t	(Hassing et al., 2019)
pGGkp046	*cat* ColE1 *ScFBA1*t	This study
pGGkp048	*cat* ColE1 *ScGPM1*t	(Hassing et al., 2019)
pGGkp062	*aphA* ColE1 *SkADH1*p	(Hassing et al., 2019)
pGGkp063	*aphA* ColE1 *SkTDH3*p	(Hassing et al., 2019)
pGGkp064	*aphA* ColE1 *SkPDC1*p	(Hassing et al., 2019)
pGGkp065	*aphA* ColE1 *SkFBA1*p	(Hassing et al., 2019)
pGGkp074	*cat* ColE1 *SePDC1*p	(Hassing et al., 2019)
pGGkp096	*cat* ColE1 *ScHXK2*p	GeneArt
pGGkp103	*cat* ColE1 *ScPFK2*t	(Hassing et al., 2019)
pGGkp117	*cat* ColE1 *ScPYK1*p	(Wronska et al., 2020)
pUD565	*cat* ColE1 *GFP*	(Hassing et al., 2019)
pUD661	*bla* ColE1 *EcacpP*	GeneArt
pUD662	*bla* ColE1 *EcacpS*	GeneArt
pUD663	*bla* ColE1 *EcbioC*	GeneArt
pUD664	*bla* ColE1 *EcfabB*	GeneArt
pUD665	*bla* ColE1 *EcfabG*	GeneArt
pUD666	*bla* ColE1 *EcfabZ*	GeneArt
pUD667	*bla* ColE1 *EcfabI*	GeneArt
pUD668	*bla* ColE1 *EcbioH*	GeneArt
pUD669	*bla* ColE1 *EcbioF*	GeneArt
pUD671	*bla* ColE1 *EcfabD*	GeneArt
pUD978	*bla* ColE1 *SkADH1p-EcfabD-ScADH1*t	This study
pUD979	*bla* ColE1 *SkTDH3p-EcbioC-ScTEF2*t	This study
pUD980	*bla* ColE1 *SkPDC1*p-*EcfabB-ScPYK1*t	This study
pUD981	*bla* ColE1 *SkFBA1*p-*EcfabG-SCfBA1*t	This study
pUD982	*bla* ColE1 *SePDC1*p-*EcfabZ-ScPDC1*t	This study
pUD983	*bla* ColE1 *ScENO2*p-*EcfabI-ScPFK2*t	This study
pUD984	*bla* ColE1 *ScPYK1*p-*EcbioH-ScPGI1*t	This study
pUD985	*bla* ColE1 *ScPFK2*p-*EcbioF-ScTPI*t	This study
pUD986	*bla* ColE1 *ScPGI1*p-*EcacpP-ScGPM1*t	This study
pUD987	*bla* ColE1 *ScHXK2*p-*EcacpS-ScTDH3*t	This study
pUDP145	*bla* ColE1 panARS(OPT) *hph ScTDH3*p-HH-gRNA$_{ScSGA1}$-HDV-*ScCYC1*t *AaTEF1*p-Sp*cas9*$^{D147Y\ P411T}$-*ScPHO5*t	(Wronska et al., 2020)
pUDR119	*bla* ColE1 2µ *amdS ScSNR52*p-gRNA$_{ScSGA1}$-*ScSUP4*t	(Papapetridis et al., 2018)
pUDR244	*bla* ColE1 2µ *amdS ScSNR52*p-gRNA$_{ScBIO1}$- *ScSUP4*t	(Wronska et al., 2020)
pUDR791	*bla* ColE1 2µ *amdS ScSNR52*p-gRNA$_{EcBioF}$-*ScSUP4*t	This study
pROS11	*bla* ColE1 2µ *amdS ScSNR52*p-gRNA$_{CAN1}$-*ScSUP4*t-*ScSNR52*p-gRNA$_{ADE2}$-*ScSUP4*t	(Mans et al., 2015)
pROS13	*bla* ColE1 2µ kanMX *ScSNR52*p-gRNA$_{CAN1}$-*ScSUP4*t-*ScSNR52*p-gRNA$_{ADE2}$-*ScSUP4*t	(Mans et al., 2015)

946

947

948 Table 3 | List of primers used in this study.

Primer no.	Sequence 5' → 3'
1719	TCCATCCGGTCTTTATCGAC
7469	GGAGTTGACCGTCTTAACAG
9630	AAGCATCGTCTCATCGGTCTCAAACGTATTCTTAGTGGATAACATGCG
9631	TTATGCCGTCTCAGGTCTCACATATTTTAGGCTGGTATCTTGATTC
10320	CATGCGCGGATGACACGAAC
10325	AGTCATCCGAGCGTGTATTG
10757	AAGCATCGTCTCATCGGTCTCAATCCGTTAATTCAAATTAATTGATATAGTTTTTTAATG
10758	TTATGCCGTCTCAGGTCTCACAGCCGCGAACTCCAAAATGAGC
10765	AAGCATCGTCTCATCGGTCTCAATCCGATTAATATAATTATATAAAAATATTATCTTCTTTTC
10766	TTATGCCGTCTCAGGTCTCACAGCCGGTACACTTCTGAGTAAC
10771	AAGCATCGTCTCATCGGTCTCAATCCACAAATCGCTCTTAAATATATACC
10772	TTATGCCGTCTCAGGTCTCACAGCGAAATAGGACCTGATATCCTCC
10873	ACGTGCGGAATAGGAATCTC
11898	CGCGGAAACGGGTATTAGGG
11899	CTAGATCCGGTAAGCGACAG
12223	CCAGGTGGCGTGCTAAACTTTTATAATGTATAAAAACCACCACCTCATAAAGTTTACTGGATATCATCATTTCTGCCACAAA TATATGTACTGAGTCTATACGTCAAAGTAAAAAAATAA
12224	TTATTTTTTTACTTTGACGTATAGACTCAGTACATATATTTGTGGCAGAAATGATGATATCCAGTAAACTTTATGAGGTGGT GGTTTTTATACATTATAAAAGTTTAGCACGCCACCTGG
12450	TCTGTCAGTTGGTTAAGCGCCGCTACGATTACTACACATGCCACAGACTGATCTACAATGTATCCTCCTTTTAAACAGTTGA TG
12455	ACATTGCATGGAATCAGGGCCTCAATATGTGGGAGAATGCATGAGTACGCGAGCGATCCTCCTGGTCAAACTTCAGAACTAA G
12655	TTTACAATATAGTGATAATCGTGGACTAGAGCAAGATTTCAAATAAGTAACAGCAGCAAATCCGATTTCCGTGGTTGATG
12656	CCAGGGCTCAAATGGCATAAACACTGATGGAACAGGTAGCATCGAACGTGTGTCAAACGCATGTTAGCGTCAACAACAAG
12657	GGCACAGACGAATCACTGACTGATCTGTACCACTGCGTCGACATAACTTTCCAGAAGCGCGTGGGTGCGTCAACTACATC
12658	TGAGCCAGTGCATTCCATCGATGCAGATTCGCGTCCACGTAACGTATCGGAAGCATAGGCAACAATGCCAACCCCTCTAC
12659	TGTGAGCAGTCATCCACTCGGCATAAGCCTGAATTGCACCATATCCTTGGAAGCCTGGGCGAAGCTATCTTCCGGTTATG
12660	TCCTCGACGCGATGGCATATCCAGTGTGATAACGTATGAGAAGGTACTGGAAGCTACTGCAACACTAAACGAAGGCTATC
12663	CACTGCGTGTTAAGGATATGCCTAAGGATACATGACACGCATAGCTCATTAACCGGCACGTGGATAACATGCGGCATTTC
12664	GCCGCGTAGACAATAGATCACCATCTAGTTGAATCCTGAGAGACTATCTCTAATGACCCGGGTAAAGTACAGCTACATTC
12665	GCGTTTGACACACGTTCGATGCTACCTGTTCCATCAGTGTTTATGCCATTTGAGCCCTGGACACACCGAGATTCATCAAC
12666	GCGCTTCTGGAAAGTTATGTCGACGCAGTGGTACAGATCAGTCAGTGATTCGTCTGTGCCATATACATACGCTGACATGG
12667	GCCTATGCTTCCGATACGTTACGTGGACGCGAATCTGCATCGATGGAATGCACTGGCTCATCGCCATCCTGATAATCATG
12668	GCCCAGGCTTCCAAGGATATGGTGCAATTCAGGCTTATGCCGAGTGGATGACTGCTCACATTGAAATGACTCCGCAGTGG
12669	GCAGTAGCTTCCAGTACCTTCTCATACGTTATCACACTGGATATGCCATCGCGTCGAGGATTCCTTGGTTCCACTAATTC
12674	GAAAAAACTAGATCCGGTAAGCGACAGATCTTTGAATTTGTTTATAGCCGACTCTAAGTCCAGAATCGTTATCCTGGCGG
12745	AGCGTAGATAGAAGCGTCAG
12746	TCCAGTTGGTGACGTTAAGG
12747	TCAGCACCCAAGTCTTCAAC
12749	TCCAGATAGCCCATTCGTTG
12750	ACACTACGCTTGTGCTACTG
12751	GAAGCACCAGTAACCAAAGC
12752	CGAAGCTGCTTACATCACTG
12759	ATTGGCTTACCTGGGAAGTG

12760	TGCTTTGGTTGACGGTAAGG
12761	GTCAGCCAACATACCAACAG
12762	ACGAAGTTGGTCCAGGTAAG
12763	CGATACCGTAAGCGATAGAC
12764	CGCTGCTATGAACGAATTGG
13280	GGTTGCTTTGAAGCAAAGAG
13281	TTTGCCACCAGATGTTGTTC
13283	CAGATACTGGCGATCATCCG
13284	CTTGGGTGTTATCGCTAGAG
13483	TCTCCAGGACCATCTGAATC
13545	TTTGTGGCAACATAGCCAAC
13718	CCAATGAGTCTTCACATGGCGCGTGTCATGTATCCTTAGGCATATCCTTAACACGCAGTGCGGTACACTTCTGAGTAACC
13748	CGGGTCATTAGAGATAGTCTCTCAGGATTCAACTAGATGGTGATCTATTGTCTACGCGGCTTGGCAGCCATTAAACTACG
14000	AGGATCGCTCGCGTACTCATGCATTCTCCCACATATTGAGGCCCTGATTCCATGCAATGTCAGCAAATCGTCTATATCAC
14448	CATTGTAGATCAGTCTGTGGCATGTGTAGTAATCGTAGCGGCGCTTAACCAACTGACAGACATTCTCTGCTGCTTTGTTG
17154	GCGCTGGCAGTGTTCCTGCG
17991	TCTTTCTTGTTAAAAATTTCAAGCTATACCAAGCATACAATCAACTATCTCATATACAATACGCTGCAGGTCGACAACC
17992	ATAAAATTTAAAAAATATAATTCAAAAAAATAATATCTTCATTCAATCATGATTCTTTTTCTAGTGGATCTGATATCACC
18404	GAAAAAACTAGATCCGGTAAGCGACAGATCTTTGAATTTGTTTATAGCCGACTCTAAGTCCGGTACACTTCTGAGTAACC
18405	AGGATCGCTCGCGTACTCATGCATTCTCCCACATATTGAGGCCCTGATTCCATGCAATGTATATACATACGCTGACATGG
18406	TTTACAATATAGTGATAATCGTGGACTAGAGCAAGATTTCAAATAAGTAACAGCAGCAAAATGTTAGCGTCAACAACAAG
18407	GAACAATAGAACTAGATTTAGAGACTAGTTTAGCATTGGCCAAGAACTAACCATACGCATATCCGATTAATATAATTATATA AAAATATTATCTTCTTTTCTTTATATCTAGTGTTATGT
18408	ACATAACACTAGATATAAAGAAAAGAAGATAATATTTTTATATAATTATATTAATCGGATATGCGTATGGTTAGTTCTTGGC CAATGCTAAACTAGTCTCTAAATCTAGTTCTATTGTTC
18409	TGCGCATGTTTCGGCGTTCGAAACTTCTCCGCAGTGAAAGATAAATGATCCTGGCAGGAGAAAATCAACGGTTTTAGAGCTA GAAATAGCAAGTTAAAATAAGGCTAGTCCGTTATCAAC
18418	CGTTGATTTTCTCCTGCCAG

951 # Figure Legends

952 **Figure 1 | Biotin biosynthesis pathways in *Escherichia coli* (blue), *Bacillus subtilis* (green),**
953 **cyanobacteria (red) and yeast (orange)**. The *E. coli*-derived steps for biotin synthesis (blue) start from
954 the acyl-carrier protein (AcpP), which is converted from its inactive apo-form into holo-[Acp] by the
955 holo-[Acp] synthase AcpS. The malonyl-CoA-[Acp] protein transacylase FabD (EC 2.3.1.39) uses holo-
956 [Acp] to attach the acyl-carrier protein to malonyl-CoA. The resulting malonyl-[Acp] receives a methyl
957 group by SAM-dependent activity of the malonyl-[Acp] O methyltransferase BioC (EC 2.1.1.197). The
958 four-carbon (C4) molecule is elongated by the 3-oxoacyl-[Acp] synthase FabB (EC 2.3.1.41). The
959 enoyl-[Acp] reductase FabI (EC 1.3.1.9), 3-hydroxyl-[Acp] dehydratase FabZ (EC 4.2.1.59) and the 3-
960 oxoacyl-[Acp] reductase FabG (EC 1.1.1.100) convert the product of this reaction to glutaryl-[Acp]
961 methyl ester, which is in a subsequent step further elongated by FabB. The eight-carbon (C8) molecule
962 is once more processed by FabI, FabZ and FabG. After two cycles of elongation the pimeloyl moiety is
963 complete and the pimeloyl-[Acp] methyl ester esterase BioH (EC 3.1.1.85) enzyme activity removes the
964 methyl group from pimeloyl-[Acp] methyl ester. The resulting pimeloyl-[Acp] enters after conversion
965 by an 8-amino-7-oxononanoate synthase BioF (EC 2.3.1.47) to KAPA the yeast biotin synthesis
966 (orange). The pathway is prolonged by three more enzymatic steps catalysed by the yeast enzymes
967 adenosylmethionine-8-amino-7-oxononanoate aminotransferase Bio3 (EC 2.6.1.62), dethiobiotin
968 synthetase Bio4 (EC 6.3.3.3) and biotin synthase Bio2 (EC 2.8.1.6) or in *E. coli* (blue) or *B. subtilis*
969 (green) via the adenosylmethionine-8-amino-7-oxononanoate aminotransferase BioA (EC 2.6.1.62) or
970 the (S)-8-amino-7-oxononanoate synthase BioU (EC 2.6.1.-) in cyanobacteria (red), the ATP-dependent
971 dethiobiotin synthetase BioD (EC 6.3.3.3) and biotin synthase BioB (EC 2.8.1.6) to synthesise biotin.
972 KAPA synthesis in yeast is proposed to start with pimelic acid, derived from an unknown source
973 indicated with (?). Pimelic-acid conversion towards KAPA involves two enzymes in yeast, the putative
974 pimeloyl-CoA synthetase Bio1 (EC 6.2.1.14) and the 7,8-diamino-pelargonic acid aminotransferase
975 Bio6 (EC 2.3.1.47), with one of them involving putatively oxygen in the reaction. KAPA synthesis in
976 *B. subtilis* (green) starts with the synthesis of a pimeloyl-thioester by either CoA-dependent conversion

977 of pimelic acid by the 6-carboxyhexanoate CoA ligase BioW (EC 6.2.1.14) or oxygen-dependent
978 cleavage of a long chain acyl-[Acp] by the biotin biosynthesis cytochrome 450 BioI (EC 1.14.14.46).

979

980 **Figure 2 | Expression of *E. coli* KAPA biosynthesis pathway in *S. cerevisiae*.** (A) Schematic overview
981 of genetic modifications introduced at the *ScSGA1* locus. A Cas9-induced cut in the *ScSGA1* coding
982 sequence and *in vivo* homologous recombination enabled integration of expression cassettes for ten *E.*
983 *coli* genes with different promoters (green) and terminators (yellow). Intergenic regions consisted of
984 synthetic 60-bp-homologous recombination sequences (Kuijpers et al., 2013b). (B) Bar graphs
985 representing average specific growth rates of *S. cerevisiae* strains CEN.PK113-7D, IMS0481 (evolved
986 for biotin prototrophy (Bracher et al., 2017)), IMX1859 (↑ *CfBIO1,*(Wronska et al., 2020)), IMX2035
987 (↑*Ec*KAPA pathway) and IMX2122 (*Scbio1*Δ ↑*Ec*KAPA pathway) under oxic conditions on glucose
988 synthetic medium with (+, black) and without (-, white) biotin. (C) Bar graphs representing average
989 specific growth rates of *S. cerevisiae* strains CEN.PK113-7D, IMS0481, IMX1859 and IMX2035 under
990 anoxic conditions on glucose synthetic medium with (+, black) and without (-, white) biotin. Averages
991 and deviations of the bar graphs were calculated from independent duplicate cultures. Brackets between
992 two bar graphs show the p-value, which was derived from significance testing of the difference between
993 observed growth rates by one-way analyses of variance (ANOVA) and Tukey's multiple comparison
994 test using GraphPad prism 8.2.1 software (significance threshold $p_{\text{-value}} < 5.0\text{E-}02$).

995 **Figure 3 | Laboratory evolution of the engineered biotin-prototrophic *S. cerevisiae* strain**
996 **IMX2122.** (A) Specific growth rates of anoxic sequential batch cycles [n] of strain IMX2122 (*Scbio1*Δ
997 ↑*Ec*KAPA pathway) on biotin-free medium, reactor A. (B) Specific growth rates of anoxic sequential
998 batch cycles [n] of strain IMX2122 on biotin-free medium, reactor B. (C) Bar graphs represent average
999 specific growth rates of the parental strain *S. cerevisiae* IMX2122 and evolved isolates IMS0994
1000 (evolution A IMX2122) and IMS0995 (evolution B IMX2122) on synthetic medium without biotin
1001 under oxic (+, black) and anoxic (-, white) conditions. The growth rate means and deviations of the bar
1002 graphs were calculated from biological duplicates. Brackets between two bar graphs show the $p_{\text{-value}}$,
1003 which was derived from significance testing of the difference between observed growth rates by one-

1004 way analyses of variance (ANOVA) and Tukey's multiple comparison test using GraphPad prism 8.2.1
1005 software (significance threshold $p_{\text{-value}} < 5.0\text{E-}02$).

1006 **Figure 4 | Genetic alterations of the evolved isolates IMS0994 and IMS0995 compared to the initial**
1007 **engineered strain IMX2122.** Copy number coverage plots of IMX2122 (*Scbio1*Δ ↑*Ec*KAPA pathway,
1008 black), IMS0994 (evolution A IMX2122, red) and IMS0995 (evolution B IMX2122, blue) over the
1009 whole genome (A), from position 100 to 250 kbp on CHRIX (B), from position 168 to 195 kbp on
1010 CHRIX, regions including the *E. coli* KAPA pathway *SGA1* integration site. The position of coding
1011 sequences of *E. coli* genes *fabD, bioC, fabB, fabG, fabZ, fabI, bioH, bioF, acpP* and *acpS* is indicated
1012 by red arrows (C). Histograms of fluorescence intensity of nucleic-acid-stained cells of haploid
1013 CEN.PK113-7D (orange), diploid CEN.PK122 (green), IMX2035 ((↑*Ec*KAPA pathway), grey),
1014 IMX2122 (dark grey), IMS0994 (red) and IMS0995 (blue). Vertical dashed lines indicate the
1015 fluorescence intensity of reference haploid (1n), diploid (2n) and tetraploid (4n) cells (D).

1016 **Figure 5 | Abundance of the proteins of the *Ec*KAPA pathway in IMX2122 and its derived isolates**.
1017 (A) Bar graphs representing average protein abundance [a.u.] in *S. cerevisiae* strains IMX2122
1018 ((Δ*Scbio1* ↑*Ec*KAPA pathway), black), IMS0994 (evolution A IMX2122, grey) and IMS0995
1019 (evolution B IMX2122, white) grown in synthetic medium without biotin. The protein abundance means
1020 and deviations of *Ec*FabD, *Ec*BioC, *Ec*FabB, *Ec*FabG, *Ec*FabZ, *Ec*FabI, *Ec*BioH, *Ec*BioF, *Ec*AcpP,
1021 *Ec*AcpS and *Sc*Bio2 calculated from biological duplicates are displayed. Significance of differential
1022 expression is shown with the upper brackets and the False Discovery Rate (FDR) adjusted $p_{\text{-value}}$ ($^{\text{FDR}}p_{\text{-}}$
1023 $_{\text{value}} < 5.0\text{E-}02$). (B) and (C) show dot plots representing the fold-change in protein abundance ($\log_2$FC)
1024 over the average protein concentration (logCPM) of annotated *S. cerevisiae* proteins in evolved strain
1025 IMS0994 (B) and IMS0995 (C) compared to strain IMX2122. Protein abundances with an insignificant
1026 change in expression ($^{\text{FDR}}p_{\text{-value}} > 5.0\text{E-}02$) are indicated as black dashes, protein abundances with a
1027 significant increase in expression ($^{\text{FDR}}p_{\text{-value}} < 5.0\text{E-}02$) are indicated as blue triangles and protein
1028 abundances with a significant decrease in expression ($^{\text{FDR}}p_{\text{-value}} < 5.0\text{E-}02$) are indicated as orange down-
1029 triangles (those include *Ec*FabD, *Ec*FabB and *Ec*BioC). Green diamonds represent the heterologously

1030 expressed proteins *Ec*FabG, *Ec*FabZ, *Ec*FabI, *Ec*BioH, *Ec*BioF, *Ec*AcpP and *Ec*AcpS, which were not
1031 significantly up- or downregulated.

1032 **Figure 6 | Growth of *S. cerevisiae* Ethanol Red and engineered strains expressing *E. coli* KAPA**
1033 **synthesis genes**. (A) Bar graphs representing average specific growth rates of *S. cerevisiae* strains
1034 Ethanol Red (diploid, industrial ethanol producer), IMX2555 (Ethanol Red ↑*Ec*KAPA pathway) and
1035 IMX2632 (Ethanol Red ↑ *Ec*KAPA pathway / *fabD,B bioC*Δ) under oxic conditions on synthetic
1036 medium with (+, black) and without (-, white) biotin. (B) specific growth rates of *S. cerevisiae* strains
1037 Ethanol Red, IMX2555 and IMX2632 under anoxic conditions on synthetic medium with (+, black) and
1038 without (-, white) biotin. The bars represent averages and standard deviations from two biological
1039 replicates. Statistical significance between growth rates in SMD with and without biotin, and between
1040 strains grown in the same conditions using one-way analyses of variance (ANOVA) and Tukey's
1041 multiple comparison test using GraphPad prism 8.2.1 software ($p_{\text{-value}} < 5.0E\text{-}02$) is indicated.

1042

1043 Figure 1

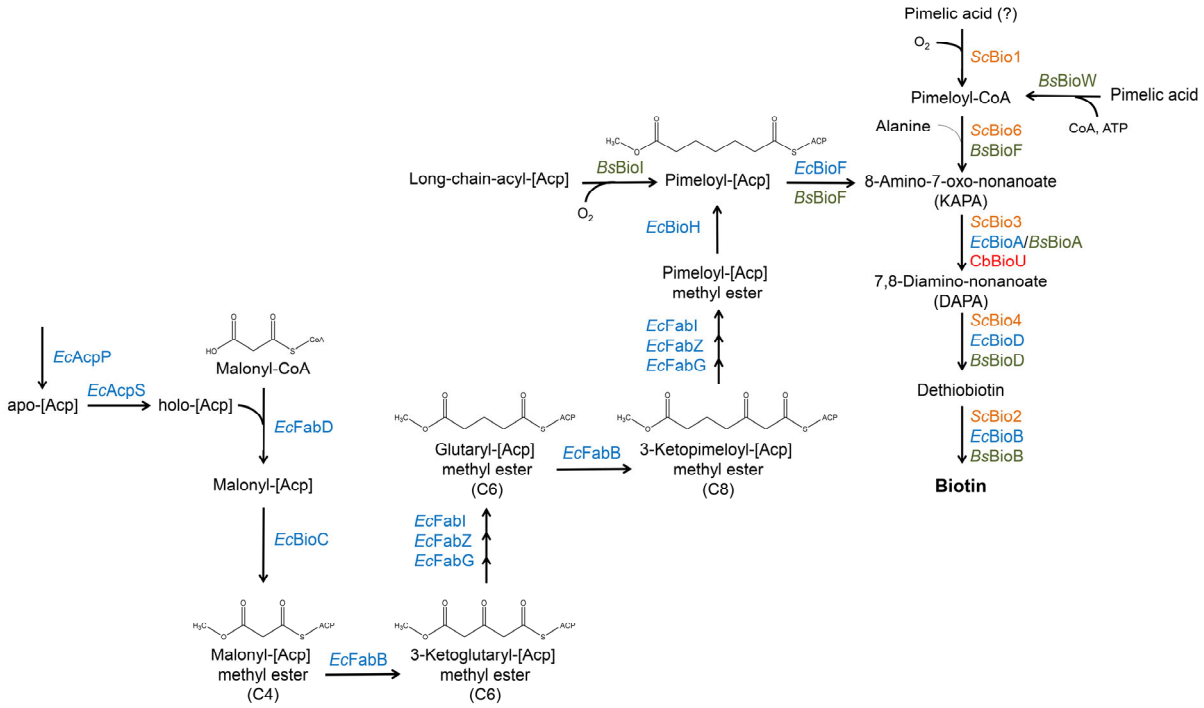

1044

1045

1046

1047 Figure 2

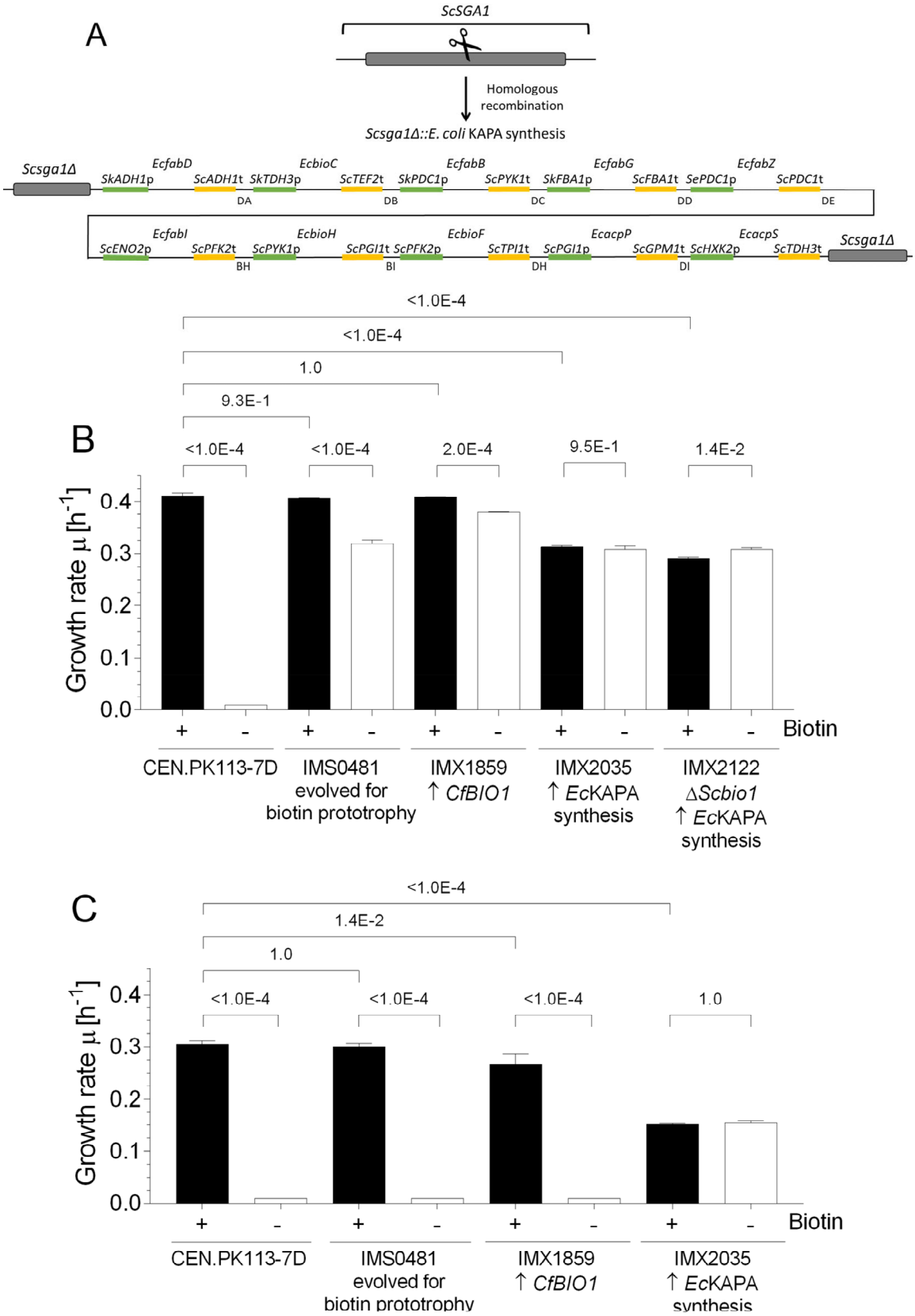

1048

1049

1050 Figure 3

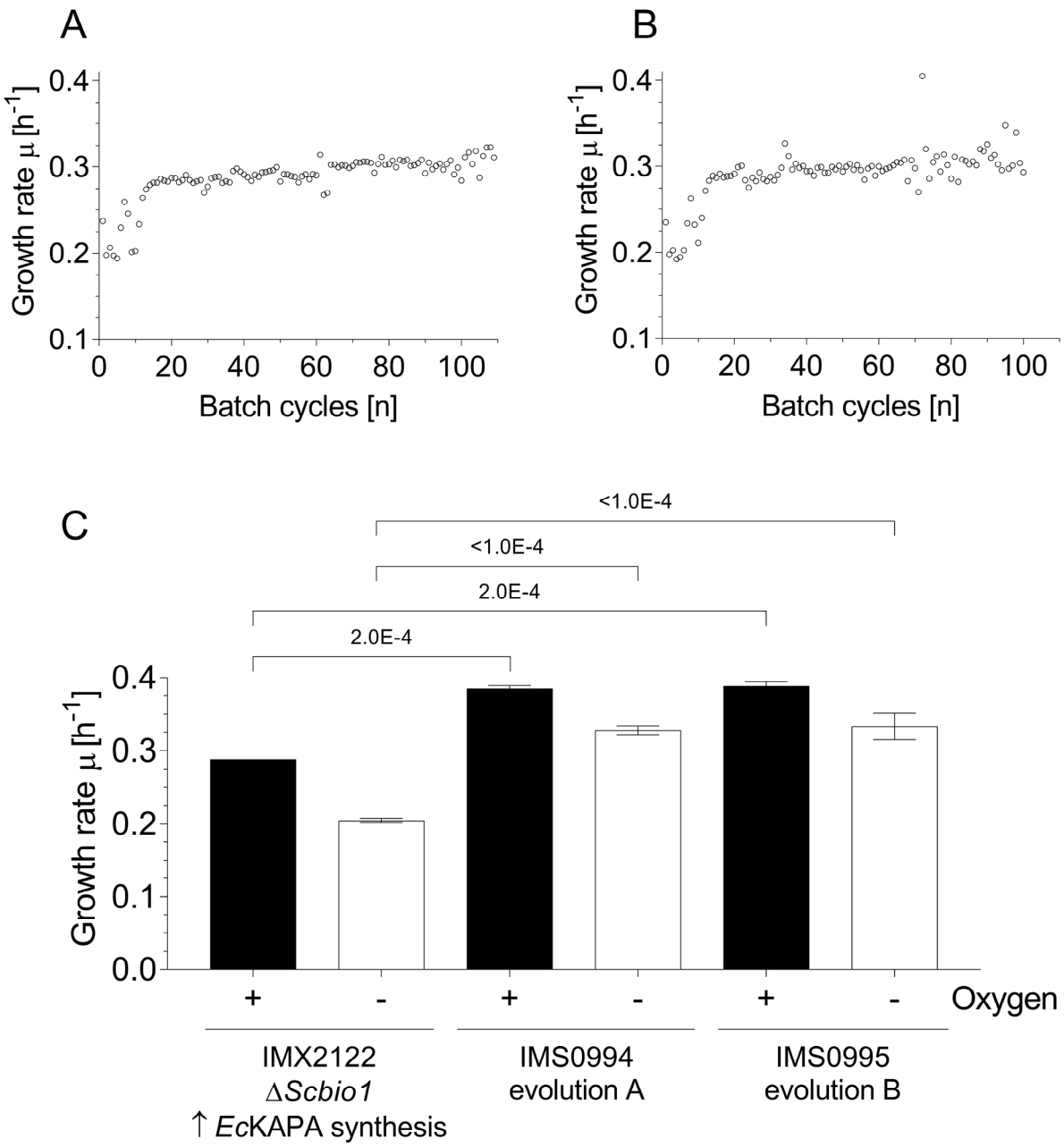

1051

1052

1053 Figure 4

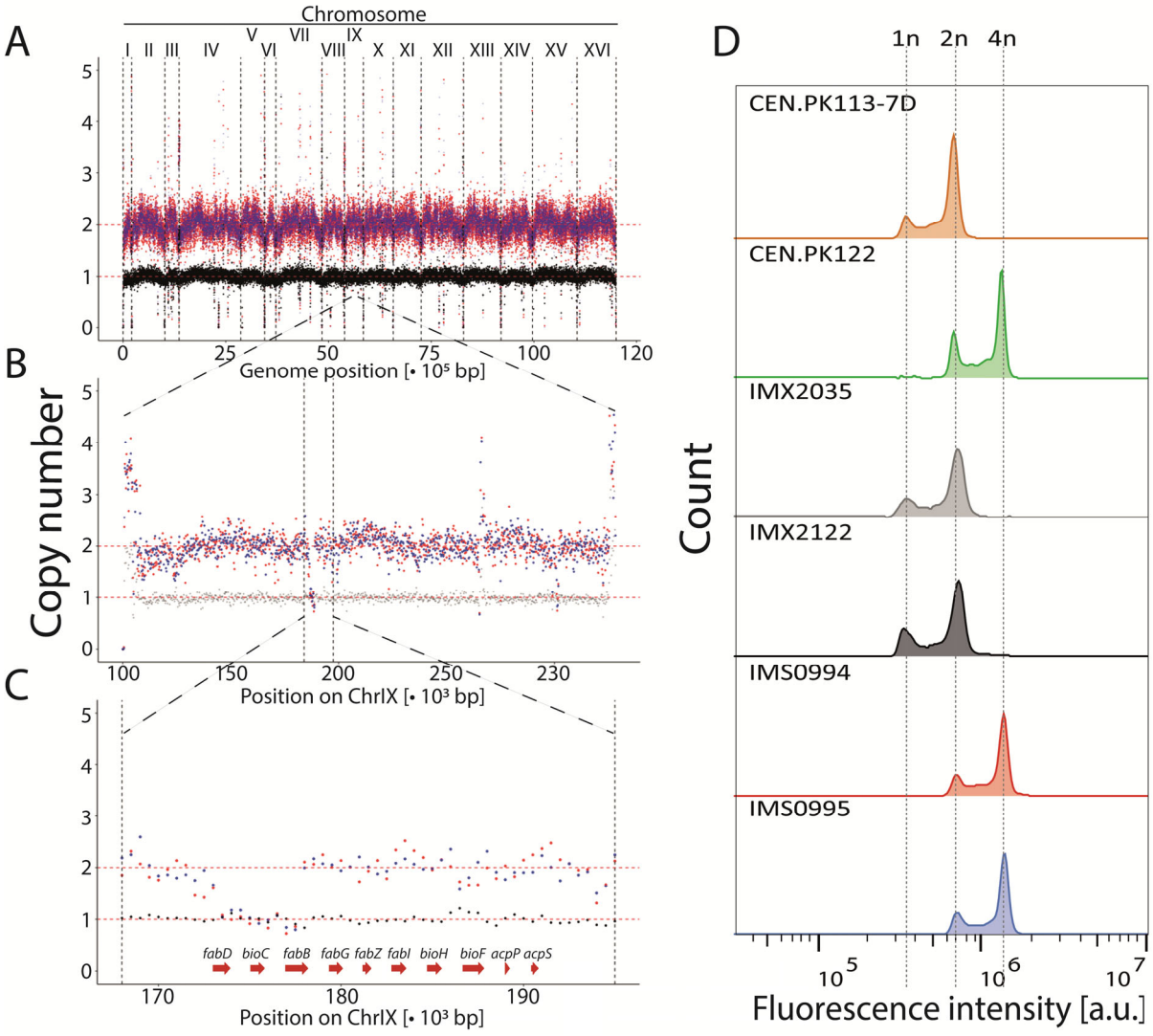

1054

1055

1056

1057 Figure 5

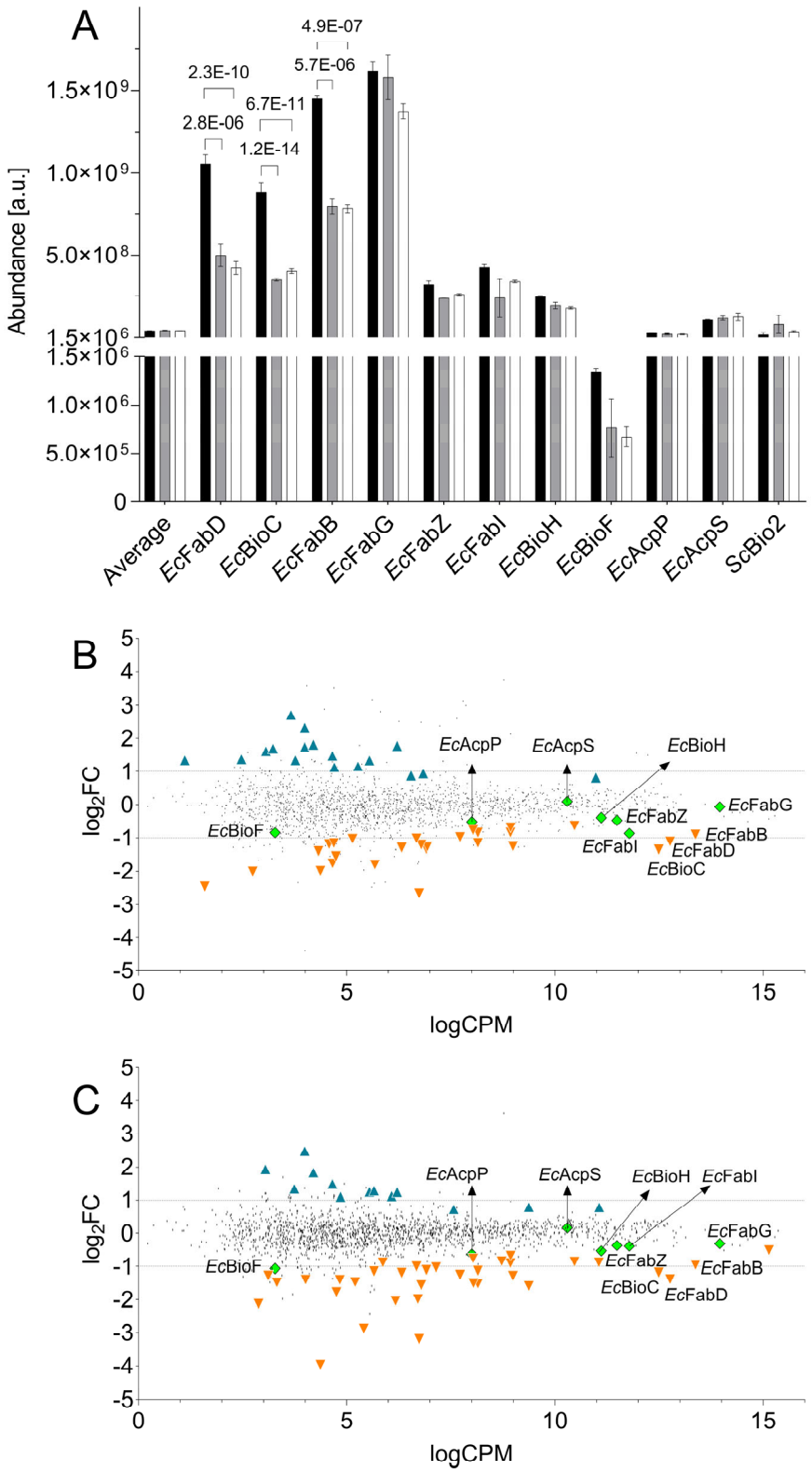

1058

1059

1060 Figure 6

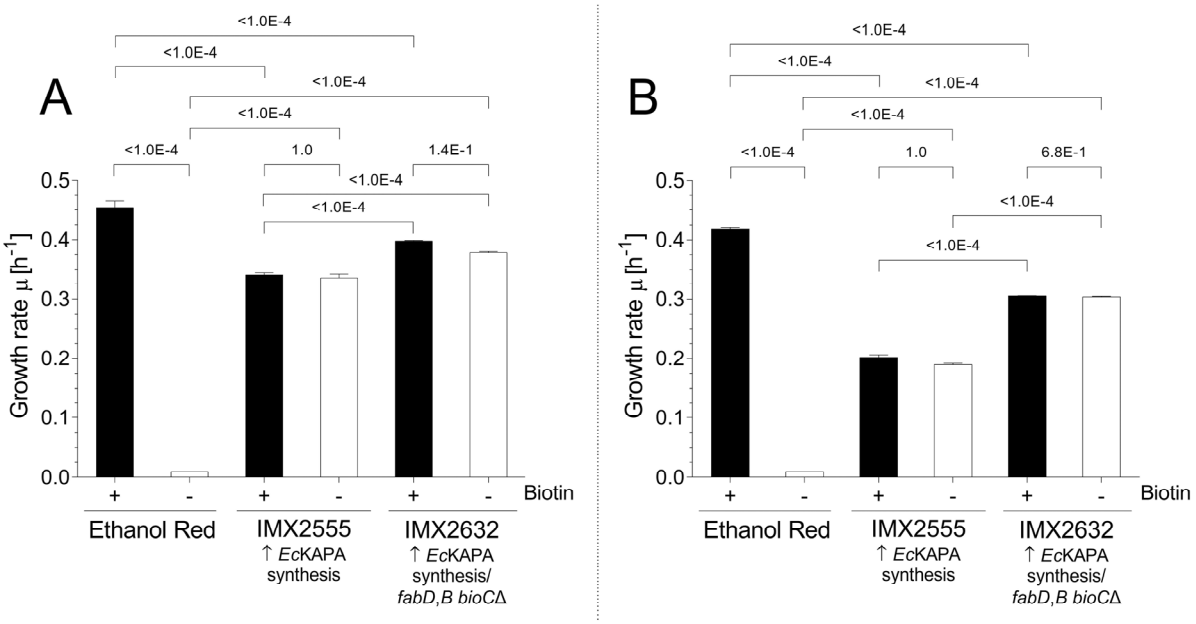

1061

1062

1063